ADVANCED ENGINEERING MATERIALS
www.aem-journal.com

Sandwich Structures with Prismatic and Foam Cores: A Review

Jian Xiong, Yuntong Du, Davood Mousanezhad, Mohamad Eydani Asl, Julián Norato, and Ashkan Vaziri**

This article provides a comprehensive review of recent research efforts on the development and characterization of sandwich structures with corrugated, honeycomb, and foam cores. The topics discussed in this review article include aspects of core-face bonding and reinforcement, enhancement of core mechanical properties and panel performance (including the role of structural hierarchy), and multifunctional advantages offered by different core constructions. In addition, the review discusses potential applications, including in morphing wing design, impact resistance, and ultralightweight applications. Future research directions are discussed.

1. Introduction

Sandwich structures are generally constructed by attaching thin stiff face sheets on the two sides of a low-density material that constitutes the panel core. This construction has the advantage of increasing the bending stiffness of the structure without adding substantial weight, and improving energy absorption and shock resistance characteristics that are not usually offered by monolithic designs.[1] The face sheets are mainly loaded in tension or compression and are usually manufactured from aluminum, steel, or composites. The core is mainly loaded in compression and shear, and is typically designed to minimize weight either through material selection, spatial distribution of matter, or both, while preserving the structural integrity of the panel under loading.[2,3] Common configurations of light-weight cores include corrugated core, honeycombs, foldcores, foam cores, and lattice cores. The area of lattice-truss cores is not discussed herein as several recent reviews on this subject have been published recently.[4–7] Common core materials include lightweight processed woods (such as end-grain balsa or plywood), lightweight metals, and polymers. Foam cores are often polymeric[8]; however, aluminum foams are used in engineering applications.[9] Prismatic cores (e.g., honeycomb and corrugated cores) are typically made from metals or fiber-reinforced composites.[10,11]

However, there are several drawbacks in the traditional prismatic and foam sandwiches, which limit their application in load bearing structures. The weak interface between the face sheets and the core of the traditional sandwich structures is one of their major drawbacks. Several studies have been carried out to strengthen the interface bonding including integrated design of face sheets and core, stitching techniques and increasing of the bonding areas.[12–15] Several technologies have been introduced for sandwich structures improving their mechanical performance and multifunctionality. For instance, foldcore addresses the anisotropy of the corrugated cores and hierarchical design increases the stiffness and strength of sandwich structures.[16,17] The hybrid design combines the merits of different sandwiches.[18] Special topological designs add innovative properties such as negative Poisson's ratio and auxetic behavior to the sandwich structures.[19] Multifunctionality is another improvement for the traditional sandwiches. Hybrid design provides new possibilities for multifunctionality combining mechanical, thermal, and electromagnetic properties.[18,20] The diversity of the possible configurations, enhanced mechanical properties, being light-weight with a high specific strength, and more importantly multifunctionality make sandwich structures a superior material choice in aerospace engineering, automobiles, marine engineering, etc.[21–27]

This review article provides a comprehensive review of the current state of the art of sandwich structures with foam based and prismatic core construction. The review includes core-face reinforcement, enhanced mechanical properties, and discussions on tailoring of properties and multifunctionality for each core type. We exclude computational design methods, as there is a wealth of published works in this area whose mention would greatly expand this review and divert from the aforementioned focus.

2. Corrugated Cores

Corrugated cores are prismatic structures that typically form open channels in one direction. The mechanical performance

Prof. J. Xiong, Dr. Y. T. Du
Center for Composite Materials and Structures
Harbin Institute of Technology
Harbin 150001, P. R. China
E-mail: jx@hit.edu.cn

Prof. A. Vaziri, Prof. D. Mousanezhad, Prof. M. E. Asl
Department of Mechanical and Industrial Engineering
Northeastern University
Boston MA 02115, USA
E-mail: vaziri@coe.neu.edu

Dr. J. Norato
Department of Mechanical Engineering
University of Connecticut
Storrs CT 06269, USA

DOI: 10.1002/adem.201800036

and structural behavior of corrugated cores have been comprehensively investigated to address issues related to core-face reinforcement, isotropic design, and their quasi-static and dynamic response to applied external loads. Several innovative designs of corrugated structures have been proposed in the past few years expanding their range of potential applications. Examples of novel core designs are integrated woven corrugated cores,[28] hierarchical corrugated cores,[29] zig-zag trapezoidal corrugated core,[30] two way corrugated cores,[31] bi-corrugated plate cores,[32] and bi-directional corrugated-strip-cores.[31] The categorization of corrugated structures is summarized in **Figure 1**, and is discussed in detail in the following sections.

2.1. Integrated Woven Corrugated Core

The integrated woven corrugated sandwich composite (IWCSC) core was developed by Jin et al.[28] with the aim of increasing face-core debonding resistance. The mechanical properties and the failure modes of IWCSCs were investigated by performing out-of- and in-plane compression, out-of-plane shear, and three-point bending tests.[28] In the compression test, gradual core crushing and the subsequent core contact with the face sheets result in a ductile load–displacement behavior.[28] The response exhibits four characteristic stages, namely, elastic deformation, buckling softening, deformation plateau, and densification. The anisotropy of the core results in different failure mechanisms of the IWCSC panel when subject to bending in different loading directions. When bent in the warp direction, the beam failed after the shear failure of the core, as shown in **Figure 2**a. When bent in the weft direction, the panel failed through indentation of the face sheets, shown in Figure 2b. No debonding failure was found in the bending experiments indicating the enhanced skin-core debonding resistance.

Russell et al.[33] studied a corrugated structure stitched to 3D woven S2-glass fiber face sheets and infiltrated with a rubber-toughened, impact-resistant epoxy. This structure combined three-dimensional woven glass fiber fabrics with z-yarn fibers to inhibit delamination. The combination of Kevlar stitching of a corrugated E-glass core to face sheets made of a high strength S2-glass fiber, along with the large contact area between the core webs and the face sheets, resulted in a robust core-face sheet attachment with high load transfer capacity. The technique was then used to fabricate a variety of corrugated core sandwich structures.[10,34,35] Kazemahvazi et al.[34] compared the quasi-static and dynamic mechanical performance of 3D-assembled (integrated woven), CFRP, and 6061-T6 beams by three-point-bending and impact. As is shown in **Figure 3**, the 3D-assembled beam outperforms the CFRP and 6061-T6 beams in flexural strength and is more than 300% and 40% higher than the 6061-T6 and the CFRP beam in energy absorption. The **Figure 4** shows the different deformation and failure mode of the three sandwich beams under impact. There is no tearing of the Al sheets in the core or face sheets and plastic buckling is found in the core of the 6061-T6 beam. Shear fracture of the core and de-bonding of the core from the face sheets exist in the CFRP beam. Fracture happens in the front face sheet of the 3D-assembled beam under the impact site, while the joint sections between the face sheet and the core remains relatively intact.

2.2. Hierarchical Corrugated Core

Hierarchical designs for corrugated cores leverage the fact that the strength of low-density corrugated cores is primarily governed by the buckling strength of the individual core members. Therefore, one way to enhance the buckling strength of the corrugated core is to introduce hierarchy, that is, fabricating individual corrugation elements themselves as sandwich panels as shown in **Figure 5**. Kazemahvazi et al.[11,36] investigated the compressive and shear response of hierarchical corrugated composite cores and compared the

Jian Xiong received his B.Sc. degree in engineering mechanics from the Harbin Engineering University in 2006, and obtained his Master (2008) and Ph.D (2012) in engineering mechanics from Harbin Institute of Technology. He is currently a full Professor at the Center for Composite Materials and Structures at Harbin Institute of Technology. His current research interests include composite structures, lightweight structures and cellular material.

Yuntong Du received his B.Sc. degree in theoretical and applied mechanics from Shandong University of Science and Technology in 2014, and obtained his Master degree in engineering mechanics from Harbin Institute of Technology in 2016. He is currently a PhD candidate at the Center for Composite Materials and Structures at Harbin Institute of Technology. His current research interests include composite materials and foldcore sandwich structures

Dr. Mohamad Eydani Asl is a Postdoctoral Research Associate at Northeastern University. He received his Ph.D. and Masters degrees in mechanical engineering from University of Massachusetts Lowell. His research encompasses experimental and analytical analysis of composite materials, granular materials and structural dynamics. He is a member of Society of Experimental Mechanics (SEM) and American Society for Composites (ASC).

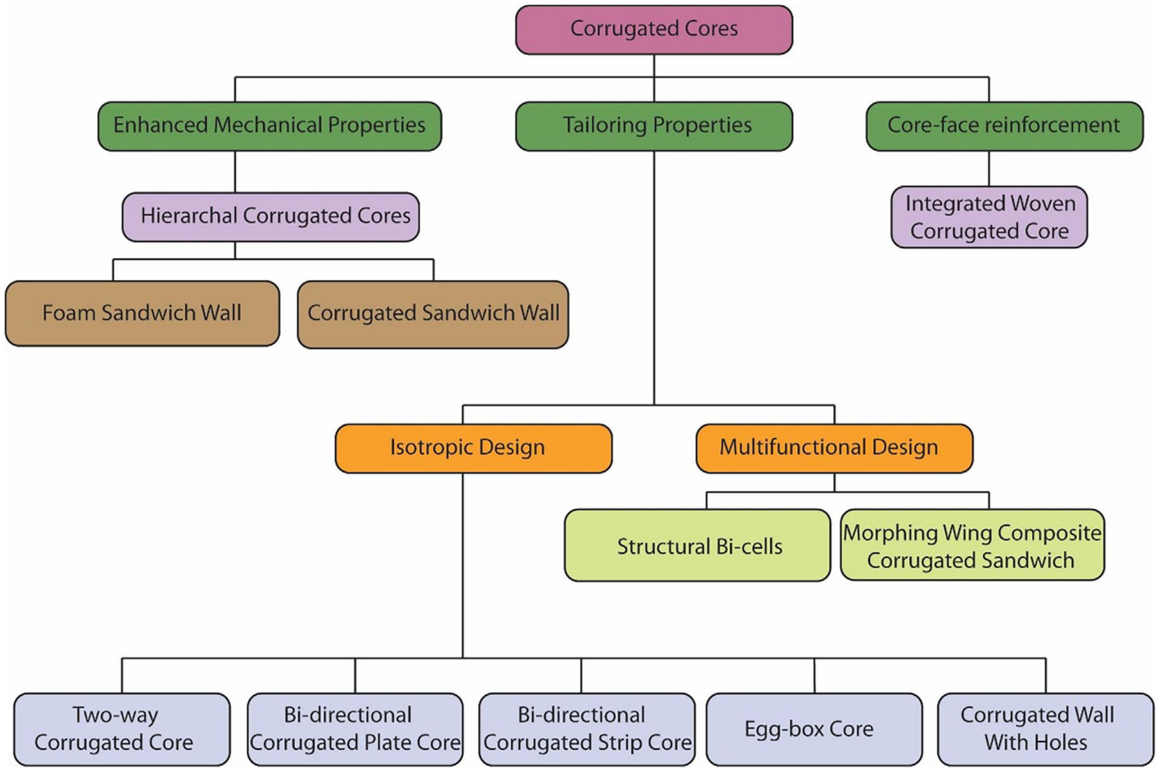

Figure 1. Categorization of the corrugated cores based on core-face reinforcement, enhanced mechanical properties, and tailoring of properties.

results with those obtained for their counterpart monolithic corrugated structures. Hierarchical corrugated cores showed improvement in the specific strength of up to seven times compared to the monolithic corrugated cores.[11] In a complementary study, Kooistra et al.[29] manufactured a second-order metallic hierarchical corrugation using sheet-metal folding and joining by dip brazing. For a relative density smaller than 5%, the second-order hierarchical structures exhibited significantly higher compressive and shear failure strengths compared to their first-order counterparts of the same mass.

2.3. Isotropic Design of Corrugated Sandwich

Corrugated cores exhibit significant in-plane anisotropy. Corrugated cores are stiff and strong in the longitudinal direction, but

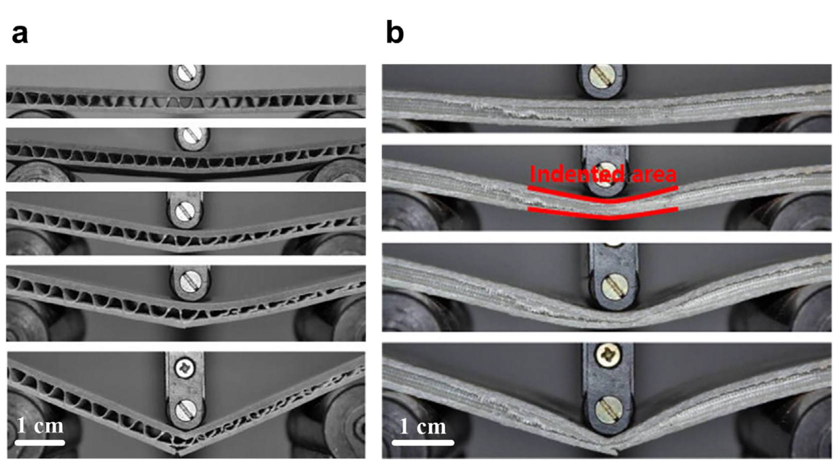

Figure 2. Failure of integrated woven corrugated sandwich composite panels under bending in a) warp direction, and b) weft direction.[28] (Reproduced with permission.[28] Copyright 2013, Elsevier).

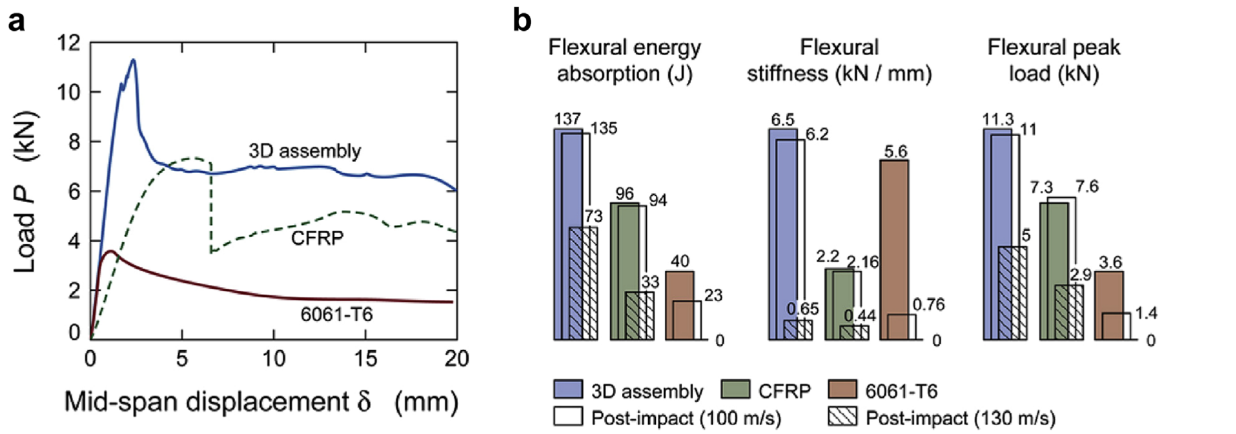

Figure 3. The comparison among 6061-T6 beam, CFRP beam, and 3D-assembled beam (integrated woven corrugated beam) subjected to quasi-static 3-point bending: a) Load versus displacement. b) Comparisons of flexural energy absorption, stiffness, and peak load.[34] (Reproduced with permission.[34] Copyright 2016, Elsevier).

weak in the transverse direction.[37–39] This significant anisotropic behavior is not always desired, and efforts have been made to create corrugated core designs with isotropic or quasi-isotropic properties. The simplest approach to achieve this is by placing corrugated cores aligned with both the longitudinal and transverse directions of the panel,[31,40] as shown in **Figure 6**. This design results in similar mechanical performance in the longitudinal and transverse directions of the panel. Leekitwattana et al.[31] proposed a bi-directional corrugated strip core (Bi-CSC) sandwich construction, shown in Figure 6b, with transverse corrugated strips that provide in-plane stiffness modulation to the sandwich plate. The transverse shear stiffness is maximum when the angle of inclined-bracing chord is larger than 63.4°.[31]

The closed unit cell of honeycomb cores and the strong anisotropy of corrugated cores limit their applications. Bi-directionally corrugated plate cores (also called foldcore) can overcome these drawbacks of traditional core construction and increase the usage of sandwich panels. Compared to the unidirectionally corrugated cores, which have three design parameters (the thickness of corrugated core wall, the height of the core, and the angle between the oblique core wall and face sheet), bi-directionally corrugated cores have two additional design parameters which influence the in-plane properties. The basic geometry of foldcores has been inspired by three-dimensional structures constructed by folding of a flat sheet of material in an origami-like manner, see **Figure 7**. Any foldable material can be used to construct foldcores, and the unit cell geometry can be designed to attain specified mechanical requirements. Foldcores can be constructed with ventilation channels in one direction. The aircraft manufacturer Airbus has undertaken the development of foldcores structures and sponsored concept studies of the next generation of aircrafts with a foldcore sandwich fuselage.[41] Many other fields of application are possible for these structures such as building insulation, engine fairings, or cargo compartments.[42,43]

Several techniques have been developed for manufacturing of foldcore sandwich structures. A discontinuous folding process in a prototype scale has been developed based on the transformable matrices that fold the sheet material into the final geometry, with a recent focus on efficient continuous manufacturing. Basily and Elsayed[44] investigated efficient continuous manufacturing processes of foldcore materials with the objective of minimizing manufacturing cost. They also tested foldcores made of kraft paper under in-plane and out-of-plane compression loads and evaluated their use as energy absorbers.[44,45] Seong et al.[32] fabricated foldcores by a sectional forming process and then bonded to the face sheets using an adhesive bond. Three-point bending tests with different core orientations in foldcore structures were conducted. Experimental results suggest that the sandwich structures with bi-directionally corrugated plate cores exhibit a quasi-isotropic bending behavior.

The weight-to-compressive-strength ratio of a foldcore is typically lower than that of a honeycomb.[46] However, foldcores made of carbon-fiber-reinforced composites (CFRCs) show compressive strength similar to a Nomex honeycomb and are lighter. This is attributed to the carbon fibers being aligned, in contrast to the random fibers in Nomex paper with lower mechanical properties. Foldcores made of unidirectional carbon fiber/epoxy prepregs were introduced by Heimbs et al.[41] to improve the performance of random fiber-reinforced aramid papers. Out-of-plane compression tests show a brittle behavior with the cell walls breaking and crushing instead of folding.

Textile-reinforced composite foldcores made from epoxy-based prepregs with woven-fabric fiber architecture, shown in Figure 7, were investigated by Heimbs.[47] It is much easier to fabricate foldcores using textile prepregs than with unidirectional prepregs owing to the stacking process. Both carbon and aramid (Kevlar) fabrics were used for the foldcore production. The mechanical behavior of composite sandwich structures with textile-reinforced composite foldcores, made by folding prepreg sheets to form three-dimensional zigzag structures, was evaluated under compression, shear and impact loads. While foldcores made of woven aramid fibers are characterized as ductile materials, carbon foldcores showed extremely high weight-specific stiffness and strength properties due to their brittle nature and absorbed energy by crushing.[47] The impact

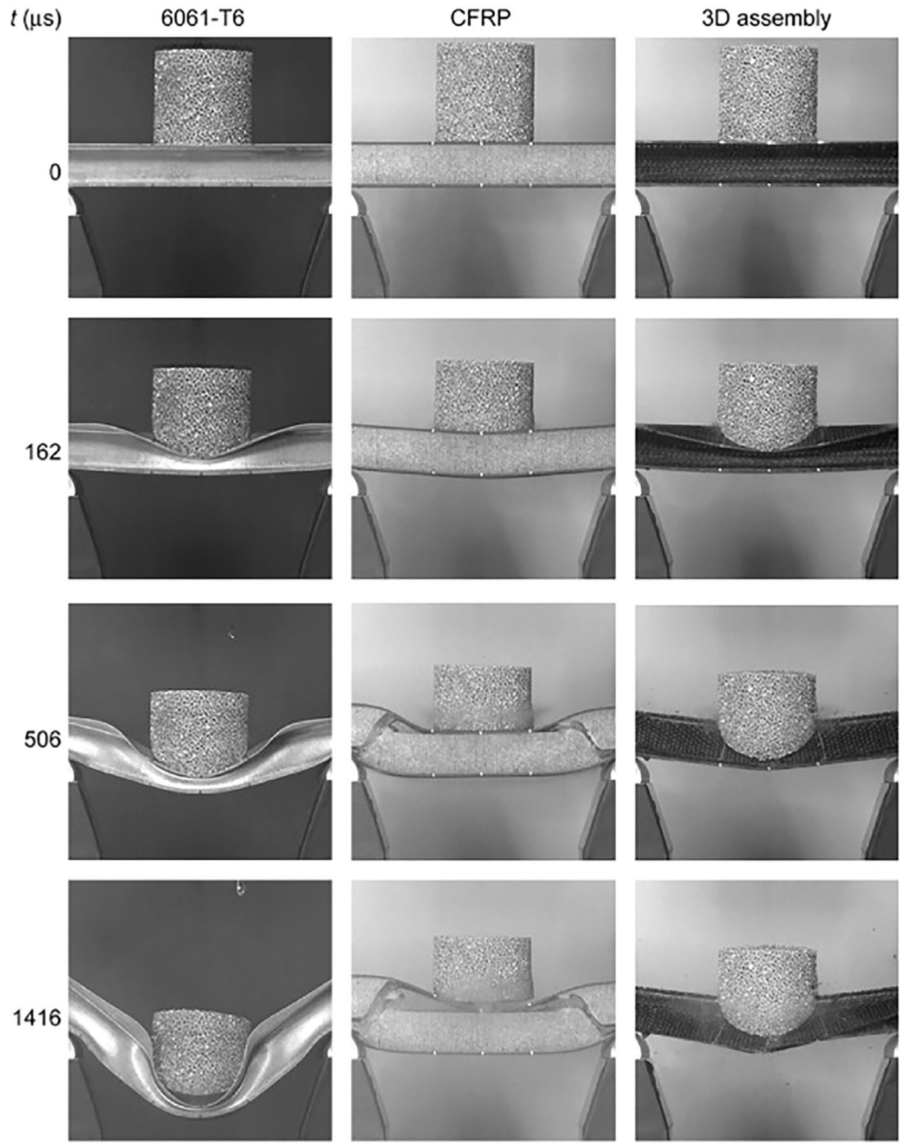

Figure 4. The comparison among 6061-T6 beam, CFRP beam, and 3D-assembled beam (integrated woven corrugated beam) subjected to foam impact at $v_0 = 130\text{ms}^{-1}$.[34] (Reproduced with permission.[34] Copyright 2016, Elsevier).

damage under low and high velocity impact loads tended to be highly localized. In addition to regular single-core sandwich structures, a dual-core configuration with two types of foldcores was also investigated, which showed a two-phase energy absorption behavior. The deformation images of single-core and dual-core configuration with two types of foldcores subjected to different low velocity impact loads are shown in **Figure 8**. The carbon foldcore crushes very locally under the impact point,

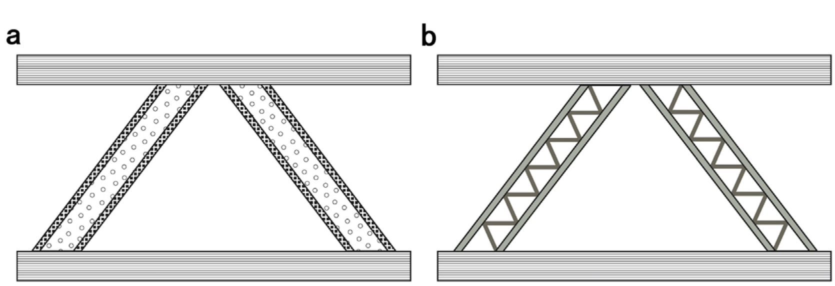

Figure 5. a) Hierarchical corrugation with foam core. b) Hierarchical corrugation with corrugated core.

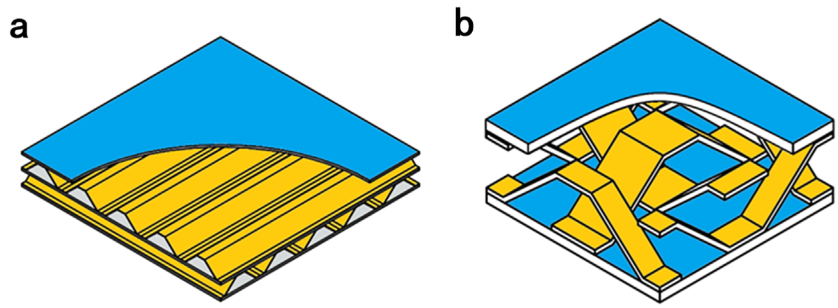

Figure 6. a) Sandwich panels with two-way corrugated core. b) Bi-directional corrugated-strip cores.

while the aramid foldcore is compressed in a ductile manner. Delamination is the main failure mode existed in the face sheet. The damage of the panel is limited to a small region as the neighboring foldcore cells stop the propagation of delaminations and the bending deformation of the upper skin.

To achieve maximum energy absorption at a given peak stress, the panel should exhibit ideally plastic behavior, undergoing large strains before final failure at a given maximum allowable stress. For open cell periodic cellular structures, foam can be used to fill the cavities of the core to enhance the energy absorbing function. A new type of composite egg-box sandwich panel was made using polyurethane foams which completely filled the cavities of the composite egg-box core. The foam-filled composite egg-box sandwich panels demonstrated a good energy absorption capacity with a stable collapse response resembling an ideal energy absorber.[48]

2.4. Multifunctional Design of Corrugated Sandwich

2.4.1. Structural Bi-Cells

A bi-cell is a single integrated battery that incorporates two electrochemical cells. The cells share one common electrode, either the anode or cathode, which is sandwiched between two of the other electrodes. The carbon fibers act as the intercalation compound for lithium ions; however, because they are partially reinforced with resin, they also provide considerable structural support. Because the fibers pass in and out of the matrix, the entirety of the carbon cathode can intercalate lithium even if the fiber mat is almost entirely reinforced as only one face of the cathode needs to be free of resin. Flat bi-cells have been constructed with general reinforcement and sandwich core components at the University of Southampton, with vibration testing being undertaken for dynamic characterizations.[49,50] Boundless Corp. manufactured corrugated bi-cells named PowerCore in order to make honeycomb cores entirely from structural bi-cell materials. The designed structural bi-cell core requires only one electrical connector per bi-cell strip, which means that the technology could be applied to large structures without significant increase of components such as electrical connectors.

2.4.2. Morphing Wing Composite Corrugated Sandwich

In the development of new aircraft, morphing wings that can change their shape via actuation are an active research topic. To develop a morphing wing, a flexible skin and a lightweight core construction is required. A possible design for the flexible skin is the use of corrugated laminates. Thill et al.[27] summarized the design possibilities for such flexible skins. Gandhi and Anusontiinthra[51] pursued several studies on the requirements of the flexible skin. Their studies showed that a highly anisotropic structure needs to be used because the skin has to be compliant in the chord-wise direction and stiff in the span-wise direction. The corrugations increase the stiffness in the weft direction, whereas the stiffness decreases in the perpendicular direction. Another study showed that the aerodynamic performance is highly dependent on corrugation amplitude, wavelength, gradient (combination of amplitude and wavelength),

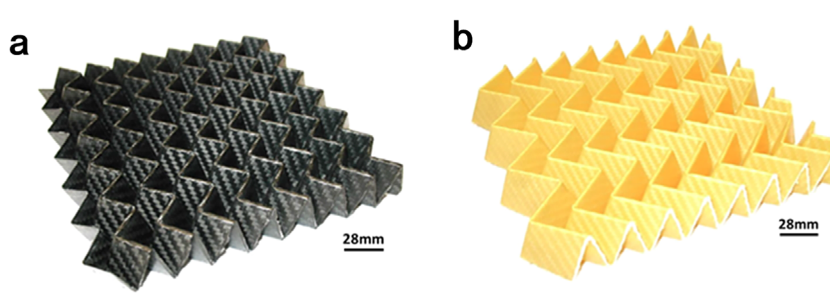

Figure 7. a) Composite foldcore structures made of carbon fabric. b) Composite foldcore structure made of aramid fabric.[47] (Reproduced with permission.[47] Copyright 2010, Elsevier).

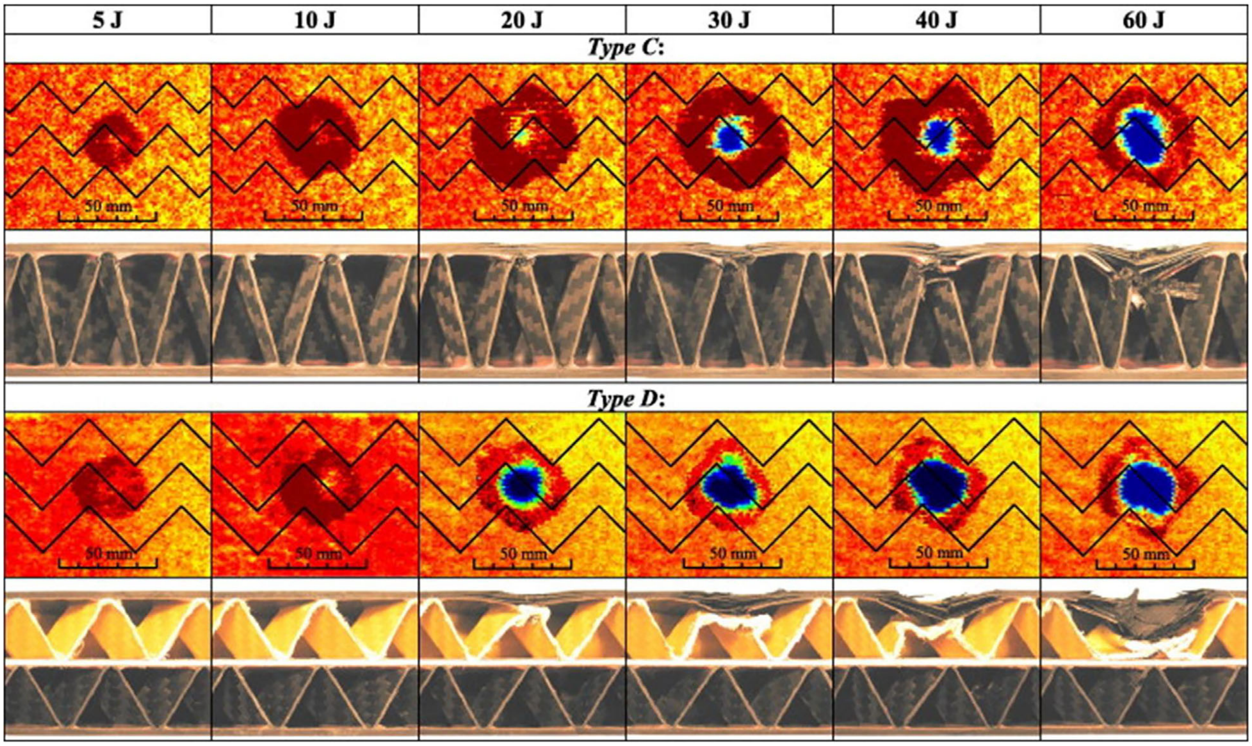

Figure 8. The failure modes of the single-core and dual-core foldcore structures subjected to low velocity impact.[47] (Reproduced with permission.[47] Copyright 2010, Elsevier).

and Reynolds number.[27] The high anisotropy between the corrugated direction and the perpendicular direction makes composite corrugated structures potential morphing skin panels (MSPs) in the trailing edge region of the morphing wings. Thill et al.[26] showed that the MSP concept exploiting corrugated sandwich structures can be successfully implemented in local morphing wing skins for low speed and small air vehicles.

Dayyani et al.[52] used experimental, numerical, and analytical methods to study the tensile and flexural characteristics of a composite corrugated core made of glass fibers. They used rubber-coated composite corrugated panels for use in morphing skins, as shown in **Figure 9**. Although significant efforts have been devoted to research into adaptive structures and morphing aircraft, examples of practical solutions are still very few. Dayyani et al.[53] studied the tensile, hysteresis and flexural performance of coated composite corrugated cores by means of numerical and experimental investigations. They proposed two concepts to improve the non-smooth surface of the panel during bending.[53]

Figure 9. The coated corrugated core used in the airfoil morphing structure.[24] (Reproduced with permission.[24] Copyright 2013, Elsevier).

The non-smooth surface of the panel in the bending mode is the main aerodynamic disadvantage of such structures in morphing applications.

Two analytical solutions based on Castigliano's second theorem are presented by Dayyani et al.,[24] which render the relationship between the equivalent tensile and bending flexural properties in both the longitudinal and transverse directions, and the geometric parameters of the coated corrugated core. In the experimental part, both coated and uncoated corrugated cores were studied in tensile and three-point bending tests. The reported coated-to-uncoated ratios of the in-plane and out-of-plane stiffness were 2.28 and 2.14, respectively. The experimental results provide a better understanding of the mechanical performance of the coated-composite corrugated panels as candidates for morphing wing applications.

3. Modern Honeycombs

3.1. Definition of Honeycomb Core Materials

Honeycomb core materials are the oldest and most common class of prismatic lattice structures, and as opposed to corrugated cores, they are usually closed-cell structures. The traditional geometries for honeycomb cores include hexagonal, square, and grids honeycombs. However, several innovative designs have been developed in the past few years.[14,15,54] The mechanical performance of modern honeycomb cores has been investigated for core-face reinforcement, enhanced mechanical properties and tailored properties (e.g., honeycombs with negative

Poisson's ratio). The categorization of modern honeycomb structures, which will be discussed in detail in the following sections, is summarized in **Figure 10**.

3.2. Extended Honeycomb Cores

The production of conventional honeycomb sandwich panels requires bonding of the skins onto the thin cell walls of the core. To achieve optimal bonding, an accurate control of the glue resin viscosity is necessary. This is a critical manufacturing consideration, as the bonded area is susceptible to debonding. Thick and heavy resin layers are used in manufacturing of honeycomb sandwich panels to ensure a good resin fillet formation.

Extended honeycomb cores use an alternative concept for the core-skin bonding compared to the conventional honeycombs. The special folding pattern of the extended honeycomb provides a larger contact area with the skins. Fan et al.[14,15] developed extended honeycomb cores by following a two-step process: the first step is forming of the cell walls by deep drawing or vacuum thermoforming of a half hexagonal shape. In the second step, the webs are folded in order to create the full hexagonal honeycomb structure. The internal cell walls are bonded using internal thermal fusion and eventually the face sheets are bonded to the core. The folding of the webs can be characterized as a continuous process, leading to high efficiency and low-cost production of the honeycomb core. The extended honeycomb production line can be readily extended into a continuous sandwich material production by adding a skin bonding process step. The efficient folding technology enables the fabrication of extended honeycombs with larger core-skin bonding area than conventional honeycombs. The internal structure, shear, and flatwise compression properties of the extended honeycombs are similar to those of the conventional honeycombs.[55,56]

3.3. 2D Honeycomb Grid Cores

Han and Tsai[55] introduced interlocked grid structures with pultruded glass fiber ribs. Using unidirectional composite ribs, one could align all fibers along the rib directions so that the stiffness and the strength of the material can be more efficiently utilized. The interlocked, carbon-reinforced cores of the Kagome-grid were manufactured and tested by Fan et al.[57] Comparisons given by Fan et al.[57] showed that the carbon-fiber-reinforced grids are much stiffer and stronger than carbon foams and aluminum lattices. The mechanical behavior of the sandwich panels was tested for out-of-plane compression, in-plane compression and three-point bending,[58] and different failure modes were observed. Based on the experimental results, buckling and debonding were the dominant failure modes, and the samples with compliant skin sheets showed an improved mechanical performance.[58]

Russell et al. fabricated CFRC honeycomb sandwiches by bonding laminate face sheets to composite cores produced by sheet slotting and interlocking introduced above.[59] Experiments were conducted to characterize the out-of-plane compressive and shear properties of composite honeycombs as a function of their relative density, cell height-to-width ratio, and number of cells in the specimen. The measurements show that the mechanical properties are only slightly sensitive to the cell height-to-width ratio and the number of cells in the specimen, but strongly dependent on the material type and fiber orientation. The experiments and analytical predictions indicate that composite cellular materials with a square honeycomb topology have high specific strength at low densities, offering new probabilities for lightweight, high-strength structural design.[59]

Eight geometric configurations of composite sandwich beams with square honeycomb cores, made of CFRC, were designed to show as many failure modes as possible. Three-point bending tests of these beams were performed in both the simply

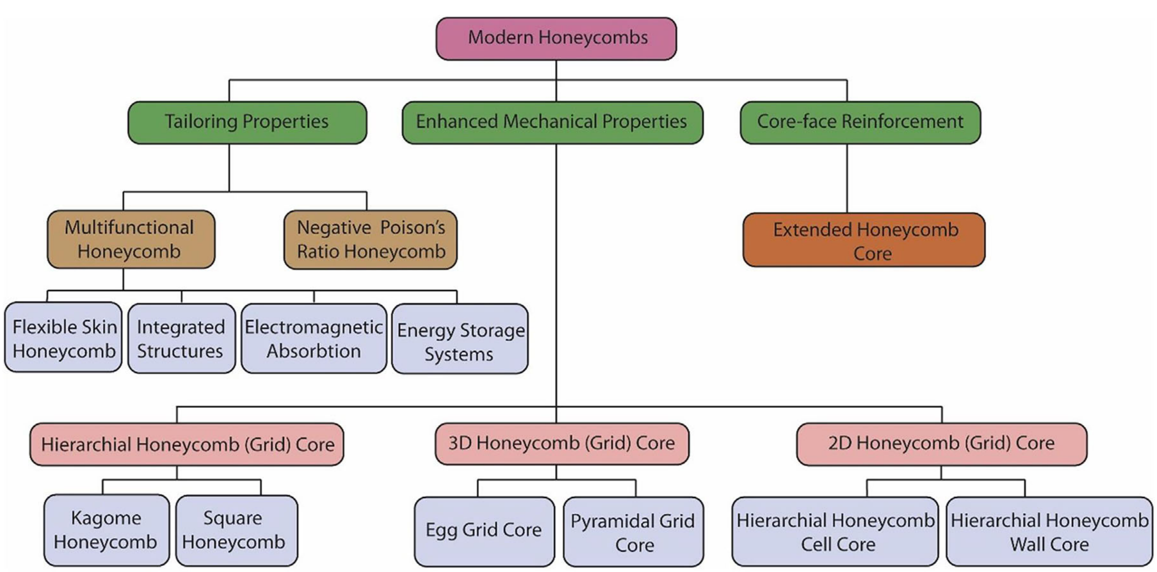

Figure 10. Categorization of modern honeycombs based on their mechanical performance.

supported and clamped configurations.[60] Analytical models were developed for the collapse loads by four types of collapse mechanisms: face microbuckling, core shear, core indentation, and face wrinkling. The first three types were observed in the eight different sandwich beams. Finite element (FE) simulations of the three-point bending responses of these beams were also conducted by constructing an FE model with unidirectional plies laid in appropriate orientations. The initiation and growth of damage in the laminates were included in the FE calculations. The constitutive model developed by Matzenmiller et al.[61] and Hashin[62] for the initiation and progressive failure in unidirectional fiber composites was verified by tensile and compressive tests on the composite material sheets. With this model, the FE analysis was able to predict the measured load-versus-displacement response and the failure sequence in each of the composite beams.

Genetic algorithm was used by Fazilati and Alisadeghi[63] to design and optimize the honeycomb structures in order to maximize the energy absorption capacity under axial impact load. The results showed that all the design requirements including the absorber size and the maximum shock could be met by using the multi-layer configuration and the energy absorption capability could be improved. The energy absorption capacities of single- and double-layer honeycomb sandwich structures were compared by Palomba et al.[64] via low-velocity impact tests, which showed that double-layer honeycomb with different cells dimensions and core arrangement could be designed to improve the energy absorption performance.

3.4. Hierarchical Honeycomb Cell Core

Ajdari et al.[65] studied analytical, numerical and experimental aspects of the mechanical properties of 2D hierarchical honeycomb structures. Replacing every vertex of a regular hexagonal honeycomb with smaller hexagons constructs a structure with one level of hierarchy. This modification builds a fractal-appearing structure, as shown in **Figure 11**. The in-plane elastic properties (effective elastic modulus and Poisson's ratio) of these honeycombs are determined by their structural organization, and they can be defined by the ratio of hierarchical hexagonal edge length to the original hexagonal edge length. By designing the structural organization of hierarchical honeycombs, a wide range of elastic properties can be achieved. The intricate hierarchical honeycombs were difficult to be fabricated by traditional manufacturing method, while 3D printing provided an appropriate and efficient method to fabricate these structures.[22,65] Honeycombs with one-level and two-level hierarchy can be up to 2.0 and 3.5 times stiffer than the regular honeycomb of the same relative density, respectively. Correspondingly, their Poisson's ratios range from nearly 1.0 to 0.28. The work highlights the role of hierarchy on the mechanical behavior of the cellular structures, providing new possibilities for the development of lightweight high-performance cellular structures.[65]

Vigliotti et al.[66] investigated the stiffness and strength of two-dimensional lattices (honeycombs) with one, two and three levels of hierarchy. The structural configuration of the lattice cores was prescribed, while the relative density and macroscopic properties were controlled by the geometrical parameters of the unit cell at each level. A multiscale homogenization method was used iteratively at each hierarchical level to obtain the macroscopic stiffness and strength of the hierarchical lattices. The material charts that were developed for the lattice macroscopic stiffness and strength demonstrate that the ranges of these properties can be expanded as the order of structural hierarchy increases. The charts provide insight into the structural features that multiple hierarchies can incorporate into the macroscopic performance of a lattice.

A hollow-cylindrical-joint honeycomb constructed by replacing the three-edge joint of the conventional hexagonal honeycomb with a hollow cylinder was presented by Chen et al.[67] Expressions for predicting its Young's modulus, Poisson's ratio, fracture strength, and stress intensity factor were also developed. The Young's modulus and fracture strength of the hollow-cylindrical-joint honeycomb can be 76% and 303%, respectively, higher than those of conventional honeycomb of same density. The Poisson's ratio of the proposed honeycomb was comparable to that of the conventional hexagonal honeycomb.

3.5. Hierarchical Honeycomb Wall Core

Zheng[68] designed and fabricated lattice panels with a hierarchical honeycomb wall core via interlocking of woven lattice sandwich ribs, with the aim of enhancing the energy absorption performance. Compression stress–strain curves of these hierarchical lattice panels exhibit high strengths, stable

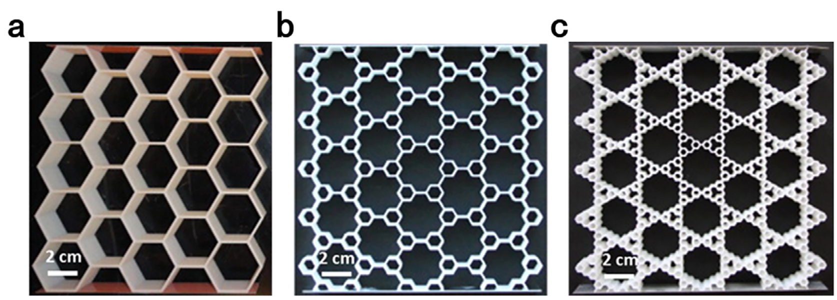

Figure 11. Hierarchical honeycombs.[65] a)The unit cell of the hierarchal honeycomb. b) The hierarchical honeycomb with 1st order hierarchy. c) The hierarchical honeycomb with 2nd order hierarchy. (Reproduced with permission.[65] Copyright 2012, Elsevier).

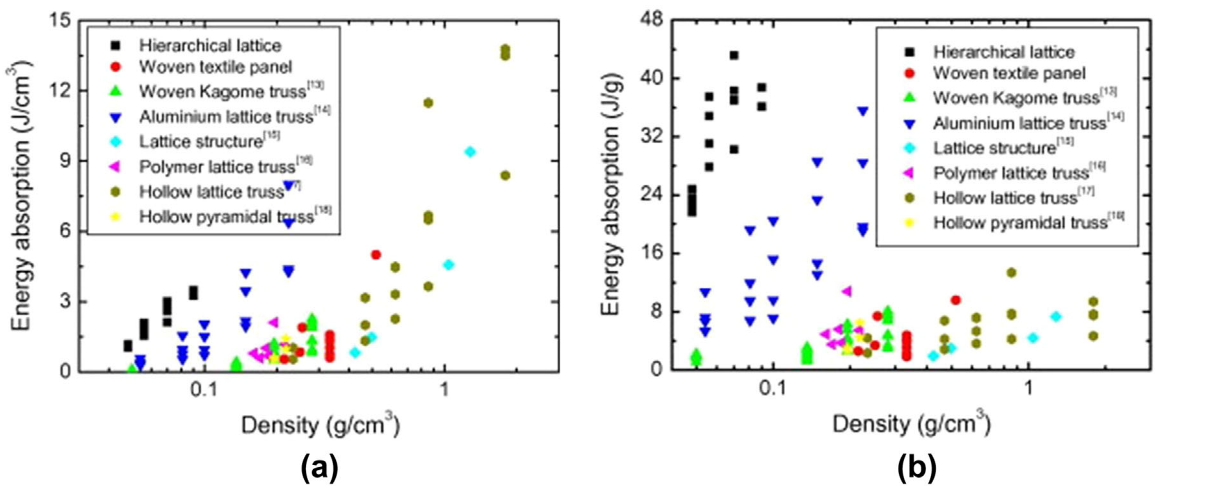

Figure 12. Comparisons among hierarchical lattice and other lattice structures for energy absorption a) per unit volume and b) per unit mass.[68] (Reproduced with permission.[68] Copyright 2012, Elsevier).

displacement plateau at a relative high stress level, and large densification strain, which is beneficial to energy absorption. A plastic model was suggested to predict the lower limits of the deformation plateau after the peak stress. It could be found in **Figure 12** and 13 that glass fiber reinforced hierarchical lattice panels have better energy absorption efficiency than other lattice panels and steel square honeycomb.

Based on the interlocking method, hierarchical composite honeycombs (HCHs) were designed, fabricated and tested by Zhao et al.[69] They showed that HCHs improve the energy absorption capability of the lightweight woven textile material.

3.6. Honeycomb Cores with Negative Poisson's Ratio

Materials with negative Poisson's ratio have been used in morphing wings and fan blades. Honeycomb cores with negative Poisson's ratio have been mainly fabricated of metal or polymeric materials.[70] Knitting technologies could be used to fabricate fabrics displaying negative Poisson's ratio effect. The special knitting method using weft yarns, warp yarns and stitch yarns produces the 3D fabric structure with negative Poisson's ratio. Also, different kinds of geometrical structures such as foldable structure, rotating rectangle and reentrant hexagon were developed to display auxetic effect.[71–73]

Numerous works have been focused on the two-dimensional auxetic structures, and many auxetic structures with different configurations including re-entrant honeycombs,[74] chiral honeycombs,[75] chiral hinge lattice,[76] star-shaped honeycombs,[77] double-arrow-head honeycombs[78,79] were presented. Those two-dimensional auxetic structures could be easily extended to three-dimensional auxetic structures, such as 3D re-entrant honeycombs,[19,80] 3D chiral honeycombs,[81] 3D double-arrow-head honeycombs,[82] etc. 3D printing provides a

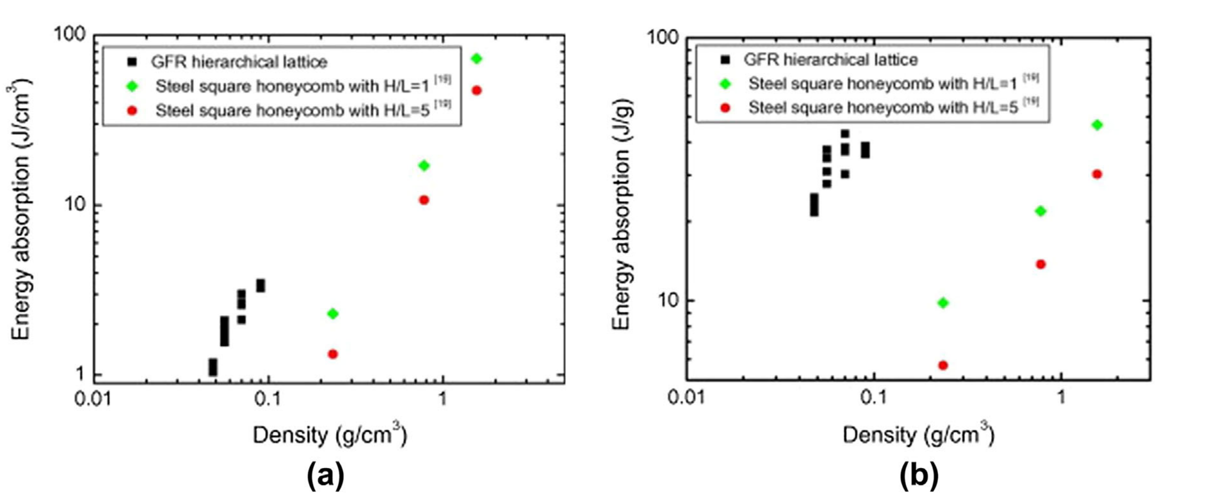

Figure 13. Comparisons between hierarchical lattice and square honeycomb for energy absorption a) per unit volume and b) per unit mass.[68] (Reproduced with permission.[68] Copyright 2012, Elsevier).

feasible and convenient method to fabricate complex auxetic structures especially for 3-dimensional auxetic materials.[80,81,83] Topology-optimized auxetic material architectures could be designed for some special purpose. The configuration with shape optimization may be complicated and irregulate such as the structure show as **Figure 14** developed by Fengwen Wang.[19] Those structures are almost impossible to be produced by traditional processing technique, which are much easier to be fabricated by 3D printing. Also, composite auxetic structures that composed of a glassy polymer as the reinforcements and a rubber-like material as the matrix were fabricated by additive manufacturing technique.[84] However, auxetic structures made of long fiber reinforced composites are still difficult to be produced by 3D printing. Traditional interlocking assembly method is a better choice.[85] Although little works were focused on the impact of auxetic structures, those structures are ideal for impact resistance and energy absorption.[78,79] The possible applications of auxetic materials including blood vessel dilator,[86] variable permeability filter,[87] auxetic piezoelectric sensor,[87] stretchable strain sensors,[88] energy absorber,[89] etc.

3.7. Multifunctional Honeycomb Cores

Cost reduction is an important factor in spacecraft design and honeycomb core materials have been successfully implemented in the structural design of the spacecraft as they offer possibilities to reduce launch costs. A multifunctional power structure design that incorporates the secondary spacecraft power supply into load carrying structures can reduce the mass and therefore the launch costs.[49]

3.7.1. Energy Storage Systems

A spacecraft structure with combined energy storage system and load carrying structure can significantly improve the efficiency of a satellite. ITN Energy Systems have introduced a series of Lithium-Ion-based batteries for use in multifunctional structures. The LiBaCore^{TM} (Lithium Battery in a Honeycomb Core) technology attaches thin-film solid state lithium batteries on the surface area of a conventional honeycomb core.[90] A different approach for the same technology combines several thin battery layers making the face sheet of a sandwich panel. To increase the power density of their batteries, ITN recently developed a solid-state lithium thin-film battery on fiber substrates (PowerFiberTM), which can be interwoven into composite materials.[91]

3.7.2. Electromagnetic Absorption

A sandwich structure with a honeycomb core filled with a carbon-nanotube (CNT) reinforced polymer foam, and with skin made of a glass-fiber-reinforced composite (GFRC), was developed by Bollen et al.[92] to enhance the electromagnetic absorption of a honeycomb sandwich with good mechanical properties. Several routes can be followed to process the CNT-filled-foam-in-a-honeycomb core, as shown in **Figure 15**. The large electromagnetic absorption performance requires a low dielectric constant and conductivity around 1 S m^{-1} to minimize the reflection and transmission of the incident electromagnetic wave.

Sandwich constructions with radar cloaking features are made from foam materials[93,94] or honeycombs. The interlocked honeycomb cores reinforced by carbon fibers of the Kagome-grid were manufactured and tested by Fan et al.[58] Multifunctional structures based on the stretching-dominated lattice grids, reinforced by glass fibers and carbon fibers, and filled with spongy materials to absorb microwaves, were designed and fabricated by Fan et al.[95] Though the density of the absorbing honeycomb panels increased, they were still much lighter than traditional absorbing coatings. The experiments suggested that honeycomb panels of 18 mm and 20 mm thickness have a better performance in radar absorption than the panels with 13 mm thickness. This method was also applied by Chen et al.[96–99] to make radar-absorbing lattice grids. Square-honeycomb and triangular-honeycomb structures were studied including the role of cell dimension and panel thickness. However, this study did not measure the mechanical properties of the sandwich panel. To combine high microwave absorption with good mechanical properties, a hybrid design based on Kagome-lattice-grid sandwich composite was developed by Yang et al.[20] The sandwich panel consists of face sheets made of fiber-reinforced composite, and honeycomb cores filled with a microwave-absorbing foam. The incident wave travels through a transparent GFRC face sheet, is absorbed by the lattice core and then reflected by the opposite CFRC face sheet. The mechanical response of these sandwich panels was measured under three-point bending and edgewise compression loading conditions. The optimal design of the skin thickness makes the hybrid panel renders comparable load capacity to the panel strengthened with

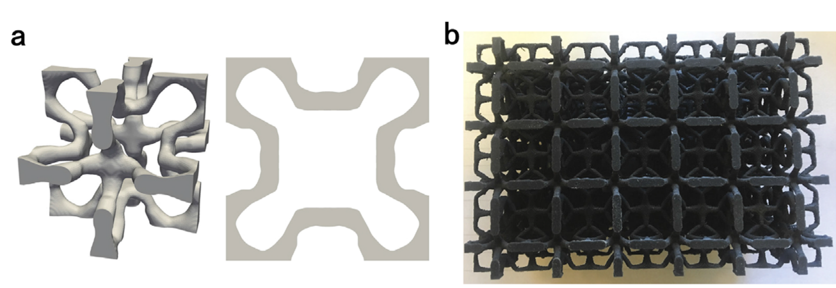

Figure 14. a) Sketch of 3D optimized nonlinear material configurations. b) Fabricated sample of the optimized material using 3D printing.[19] (Reproduced with permission.[19] Copyright 2012, Elsevier).

CFRC face sheets. Filled with microwave-absorbing foams, the composite honeycomb structure has excellent microwave absorbing properties. When using hybrid face sheets, the microwave-absorbing properties of the sandwich panels are slightly weakened compared with the microwave-absorbing foam and honeycomb, but can still meet typical requirements.

3.7.3. Integrated Structures

Conventional spacecraft structures primarily carry payload while providing space for mounted components. Multi-functional structures can additionally incorporate thermal and electronic functions. Moreover, radiation shielding capabilities can be added to spacecraft structures using multifunctional materials. By employing multifunctional structures, the fraction of the whole spacecraft volume occupied by functional devices can be dramatically increased and significant mass savings achieved. Spacecraft electronics are miniaturized and may be embedded into a structural panel thanks to the rapid development of advanced electronics such as flexible circuitry, miniaturized components, and feather-weight connectors. A typical sandwich structural panel comprises an aluminum honeycomb core and lightweight CFRP face sheets. Jang et al.[25] showed that electronics can be integrated in the panels by mounting them on a multi-layered composite enclosure. This lightweight composite enclosure provides a load-bearing structure with effective heat dissipation, radiation shielding capabilities, and an available space for embedding electronics. Environmental tests such as random vibration and vacuum thermal tests were conducted to validate the feasibility of such a multi-functional structure for use in space environments.[25]

3.7.4. Flexible Skin Honeycombs

Cellular honeycomb cores bonded to flexible face sheets have been proposed for use as flexible skins for morphing aircraft. The cellular cores, which provide underlying support to the face sheets for carrying aerodynamic loads, must have low in-plane stiffness and high in-plane strain capability. Flexible skins for morphing aircraft structures comprised of low-modulus face sheets made of high-strain materials that cover a cellular honeycomb core were proposed by Olympio et al.[100] The overall properties of the proposed skin are largely governed by the cellular honeycomb core characteristics, which are dependent on the cell parameters. The study showed that the honeycomb cores could undergo strains over ten times greater than the strain-to-failure values of conventional core materials.

4. Innovative Foam Sandwich

Sandwich composites with foam cores have emerged as a major class of lightweight structural materials in a wide range of engineering fields including aerospace, automotive, and marine structures. This is due to attractive mechanical properties such as high specific bending stiffness and high bending strength. Strong

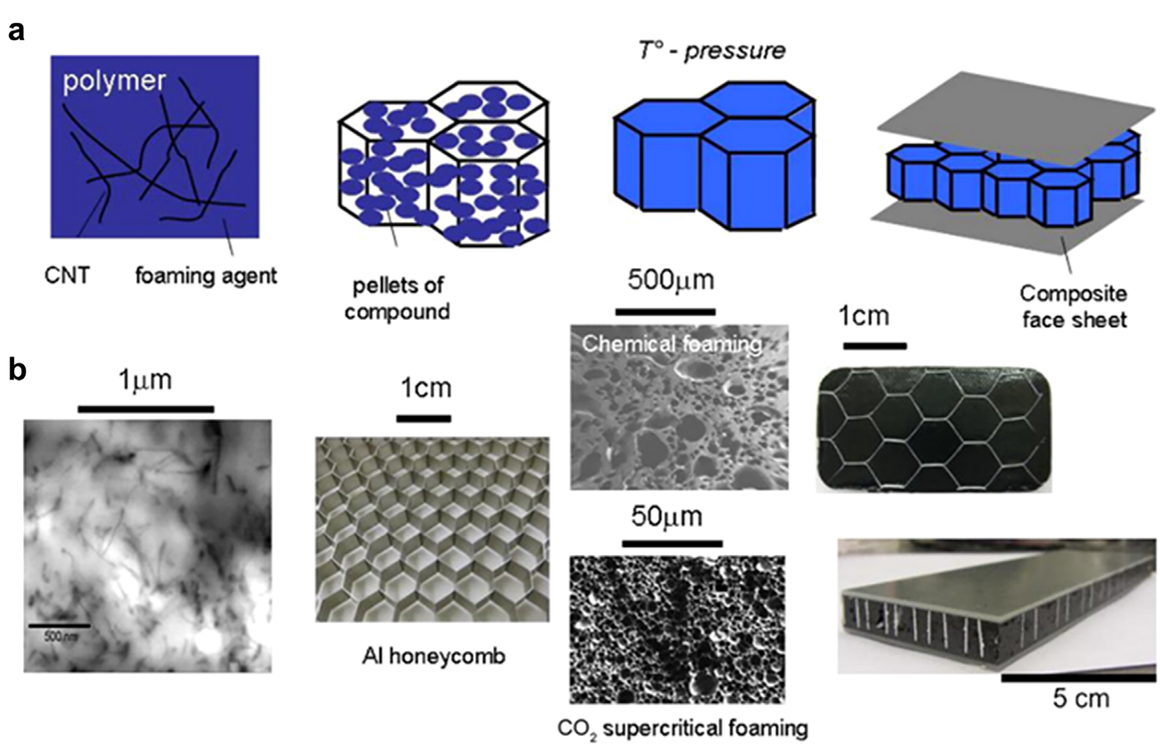

Figure 15. a) The schematic of process for manufacturing architectured sandwich panels from left to right. b) The corresponding micrographs for the materials and structures at each stage.[92] (Reproduced with permission.[92] Copyright 2013, Elsevier).

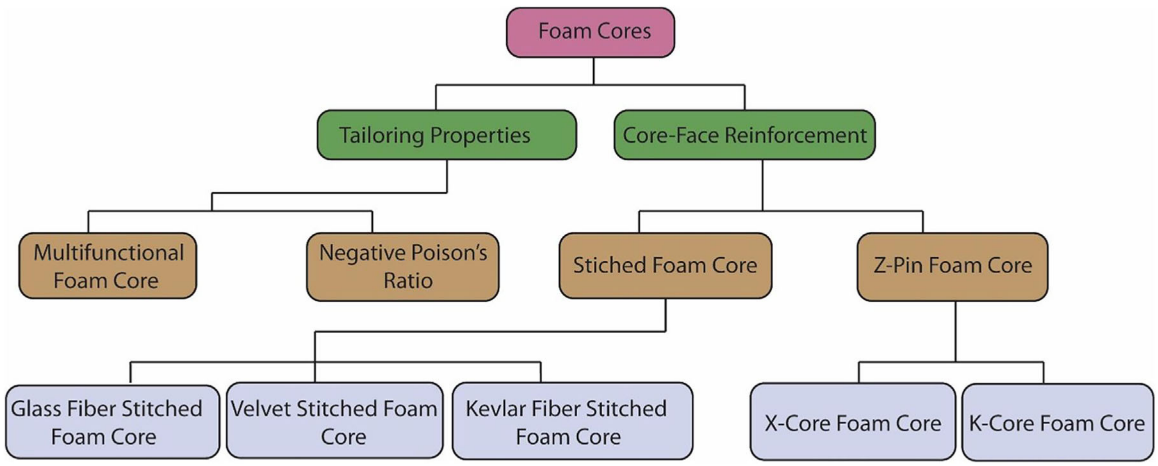

Figure 16. Categorization of novel foam cores based on their reinforcements and mechanical properties.

metallic bonding was observed for the Al alloy face sheets and cores during new integrated AFS manufacturing process.[9,21,101,102] However, sandwich structures with nonmetallic face sheets and polymer foam cores show less debonding strength compared to their metallic counterparts. Foam-based sandwich structures have been developed to improve the core-face reinforcement. In the following section, foam-based sandwich structures are reviewed.

4.1. Definition of Core Type

Stitching of monolithic composite materials has inspired the addition of transverse reinforcements in sandwich structures. Although the stitching of sandwich structures had limited applications, the bonding of the two face skins to the core material can be improved by this technique. The purpose of the reinforcement is however not only to ensure a good link between the sandwich components but also to increase the mechanical properties of this material. **Figure 16** summarizes the categorization of the foam cores with reinforcement.

4.2. Stitched Foam Core

4.2.1. Glass Fiber Stitched Foam Core

A number of studies have focused on reinforcing foam cores with glass fibers using a stitching process. An example of the fabricating process is given by Kim et al.[103] who investigated a sandwich fabricated by stitching the glass fabric and foam core material together with a stitching thread. Twisted glass and polyester threads were used to stitch together the upper and lower faces through the core. After the stitching process, an epoxy resin was infused into the stitching and then cured to form a full sandwich. The schematic of stitched sandwich panels with different stitching patterns is shown in **Figure 17**.

Bending, flatwise compression and shear experiments were conducted to compare the mechanical performance of the stitched and unstitched foam sandwich structures. The results of the shear tests are shown in **Table 1**. The shear modulus and ultimate stress of the stitched sandwiches are much higher than those of unstitched sandwich. Similar conclusions can be drawn from flatwise compression and bending tests.[104] The behavior as a function of stitching angle of stitched sandwich panels subject to uniaxial tension, interlaminar shear and bending was also investigated using finite element analysis.[105] The low-velocity impact performances of unstitched and stitched foam-core sandwich composites were investigated experimentally and numerically.[12,106,107] The impact face surface and cross-sectional view for the unstitched and stitched foam sandwich composites are show in **Figure 18**. The maximal cracking width and penetration depth of the stitched samples decrease compared to unstitched ones, which means the stitched sandwiches are able to bear a greater impact load and appear to have lower impact damage.[107] It is quite different for the mechanical behaviors of the foam core sandwiches under quasi-static loads and shock wave loads.[108–113] The unstitched and stitched foam also behave differently under blast loading. The sandwiches with unstitched and stitched foams were experimentally studied under shock wave loading by Tekalur et al. Compared to the unstitched foam sandwich, the transient load transfer through the core is much better in the stitched foam sandwiches and the imparted damage is substantially reduced.[114] Fatigue characteristics for stitched foam sandwich were also investigated. Although the stitched sandwich can increase the static bending strength considerably, the bending fatigue strength of the stitched sandwiches did not increase.[103] The Napco technology was designed by Guilleminot et al.[115] that was different from the stitching technology. The authors investigated the potential of the Napco technology process using a micromechanical modeling approach combined with a parametric probabilistic model. An experimental program was used to validate the theoretical estimates of the core-related elastic properties. It is readily shown that parts with significantly improved mechanical properties can be manufactured with the help of this technology compared to non-reinforced foam cores. Ai et al.[116] developed a structure for reentry heating corresponding to the Access to Space Vehicle. The stitched sandwich structure was modelled as a discrete stitched three-layer structure, which included the upper and lower skins, the

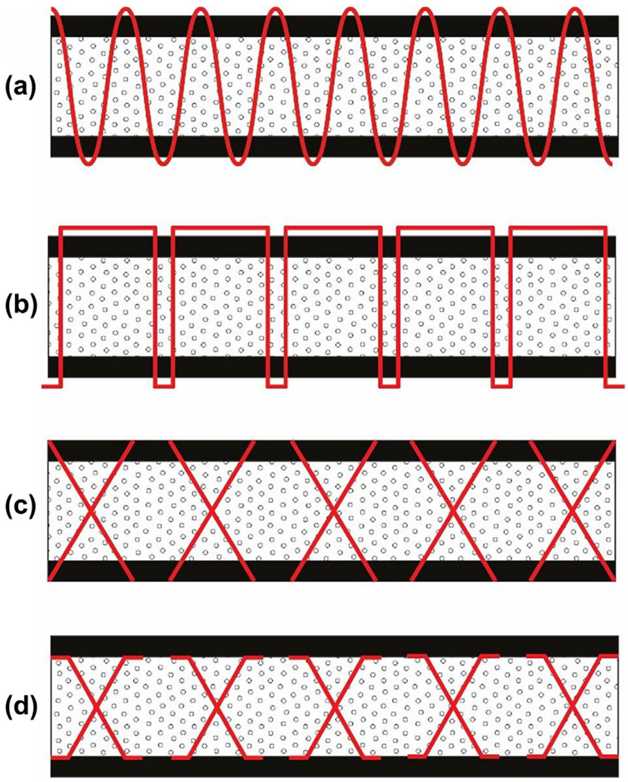

Figure 17. Schematic of stitched foam sandwich panels. a) Stitched foam core with oblique direction. b) Stitched foam core with vertical direction. c) X-Cor foam core. d) K-Cor foam core.

heat insulation core and the stitches. The three components were stitched using 2200 TEX glass yarns piercing the entire sandwich and linking the two skins through the core in a cross pattern. The ability of stitches to improve heat conductivity is limited; however, the stitches have a significant effect on the thermal stress in the stitched sandwich structures.

Since through-thickness stitching provides additional structural integrity, it has gathered particular interest for impact loading. 3-D hollow integrated cores were developed by Hosur et al.[117] and further developed to include a polyurethane foam system to fill up the hollow interstitial space.[118] Experiments and numerical finite element simulations on both the sandwich composite and its separate components were performed by Corigliano et al.[119] to characterize the out-of-plane compression and bending behavior of the highly heterogeneous sandwich material. A theoretical model was established to predict the tensile properties of 3D woven hollow integrated sandwich composites without foam filled inside. And the accuracy of the analytical model was verified by experiments and finite element analysis.[120] The low-velocity impact response of 3D-integrated-core sandwich laminates filled with and without foam, with and without additional GFRP or CFRP face sheets was investigated.[13,117,118] Vaidya et al.[121] studied the properties of stitched cores with and without foams around the reinforcing core members. They found that buckling of the core member piles and the rupture of the face sheets mainly happened in unfoamed specimens when subject to impact loading. For the foamed specimens on the other hand, core crushing along the core piles was the primary mode of failure. The foam filling supported the core piles and increased the strength of the structure by preventing buckling of core piles. A split Hopkinson pressure bar setup that consisted of an all-polycarbonate bar was used to characterize and compare the high strain-rate response of five different types of integrated-core sandwich composites in terms of the peak stress, modulus, strain at peak stress and failure modes. Foam and integrated core construction with vertical pile provide synergistic effect.[122]

4.2.2. Velvet Stitched Foam Core

These structures are made from velvet-weave sandwich-fabric preforms, rendering sandwich structures with high skin-core debonding resistance and providing the potential for low-cost sandwich construction. Compared to traditional honeycomb or foam sandwich structures, it is easier to produce delamination-resistance sandwich panels based on these structures. Judawisastra et al.[123] produced 3D sandwich fabrics using a velvet-weaving technique, and the fatigue performance of 3D woven glass-fabric/PUR-epoxy panels was investigated. The 3D woven glass-fabric/epoxy panels with polyurethane foam showed excellent fatigue performance and low stiffness degradation. De-cohesion damage was shown to play a major role in decreasing the panel stiffness. The stiffness degradation of the panel was proportional to the ratio of pile length to core properties. Pure core shear failure was not observed in three-point-bending tests or in flexural fatigue tests of 3D woven glass-fabric/epoxy panels. However, a mixed-mode failure was observed, resulting from the local buckling of the skin evolving into a local core failure area. A finite-element preprocessing program was developed by Vuure et al.[124] to predict the mechanical performance of the cores of woven sandwich-fabric

Table 1. Shear tests comparison of modulus and maximum stress for stitched and unstitched sandwiches.[104]

		Unstitched	Stitched reference	Stitched 60°	Stitched 12.5 mm
Real properties (MPa)	Maximum stress	0.20 ± 0.03	1.26 ± 0.19	0.69 ± 0.08	2.02 ± 0.52
	Modulus	3.1 ± 0.1	19.4 ± 2.3	14.8 ± 1.7	28.0 ± 2.1
Specific properties ($MPa/kg \cdot m^{-2}$)	Maximum stress	3.7×10^{-2}	20×10^{-2}	11.5×10^{-2}	24.6×10^{-2}
	Modulus	0.57	3.08	2.46	3.41

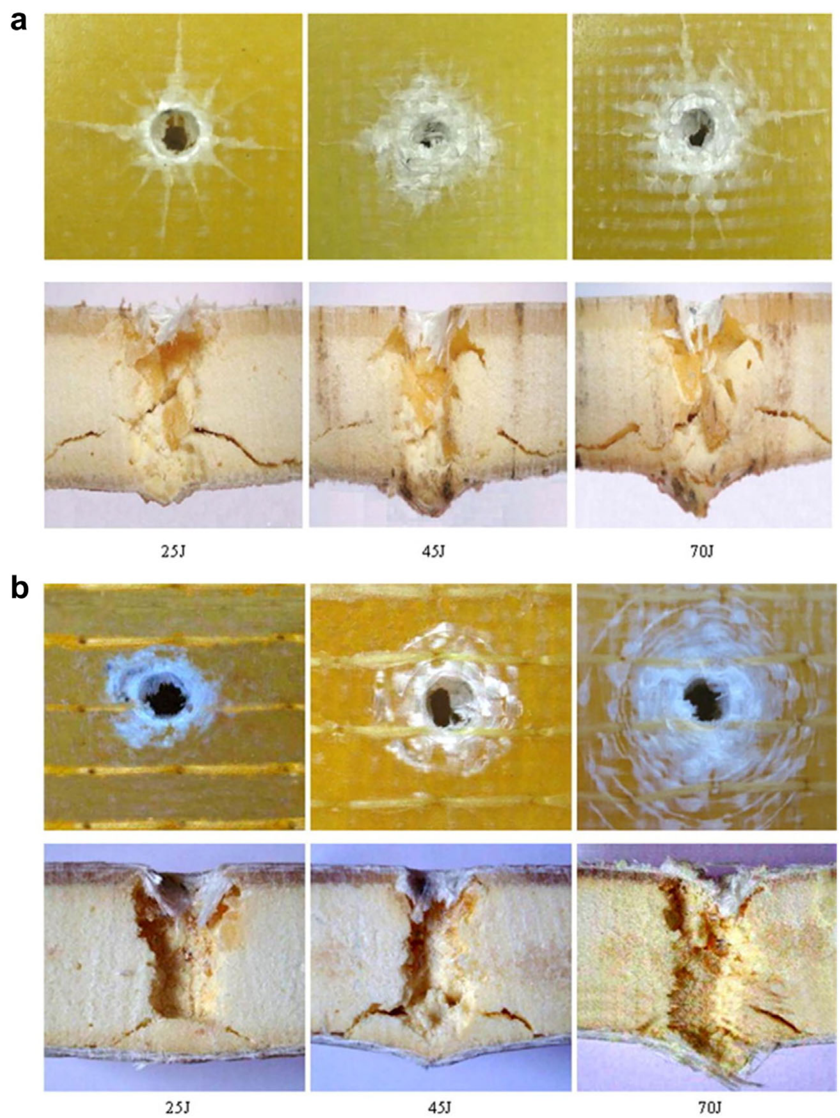

Figure 18. The impact face and cross-sectional view of failed unstitched and through-thickness stitched samples: a) unstitched samples. b) through-thickness stitched samples.[107] (Reproduced with permission.[107] Copyright 2010, Elsevier).

panels. A unit-cell of the sandwich-fabric panel representing the infinitely sized plate was determined and a detailed model that includes the shape of the piles and pillars and the distribution of the resin was developed.

Henao et al.[125] conducted a study on the effect of through-thickness tufted fibers on the compression and bending properties of sandwich structures. The tufting process also aims to prevent debonding between the skin and core by increasing the interlaminar strength and damage tolerance of sandwich structures. To evaluate the effect of tufting in sandwich structures, an experimental study was performed using edgewise compression and three-point bending tests. Tufted and non-tufted sandwich panels made of carbon/epoxy and E-glass/epoxy face-sheets, PVC and polyurethane foam cores, and Epoxy-glass through-thickness fibers with different tufting densities were tested.[125]

4.2.3. Kevlar Stitched Foam Core

Fan et al.[107] showed that, compared to unstitched samples, through-thickness stitched-foam sandwich composites are capable of bearing larger impact loads, absorbing more impact energy, exhibiting lower impact damage, and overall displaying better impact performance at the same impact energy levels. The Kevlar-fiber resin columns embedded in the stitched samples play a supporting role to help block punching, eventually delaying the rupture of stitches.

Kevlar 29 yarn was used to stitch both sets of panels because of its high strength and its successful performance in previous stitching applications with composite laminates.[126] Wang et al.[127] tested six types of stitched-foam core sandwich beam specimens with different parameters under flexural loading to study the effect of stitching density and core thickness on flexural behavior. Then, based on Eshelby's tensor and a Mori–Tanaka equivalent model, a new model is proposed to calculate the flexural rigidity of the sandwich structure, that is, in good agreement with experimental results.

4.3. Z-Pin Foam Core

Foam core sandwich structures with truss elements offer multifunctional load-bearing, energy dissipation, sound absorption, and enhanced thermal properties.[18,23,128,129] The "pin" reinforcement technology has been developed recently and is known under the commercial name of X-Cor[130] and K-Cor. In this technique, carbon-fiber or metallic (titanium or steel) pins are inserted into the foam core in the out-of-plane direction and are extended from one face sheet to the other one. X-Cor and K-Cor sandwich panels are structures composed of skins separated with a polymeric foam in which cured carbon fiber rods have been inserted in a pre-determined truss configuration. During the manufacturing process, the pins extend beyond each foam surface. In X-Cor panels, uncured face sheets are pressed on each side of the core. During the cure, the pins are entered into the face sheets. The K-Cor construction varies by the fact that the length of pins that extends outside the polymeric foam core is pressed flat on the surface of the foam by a hot-press process. The skins are then bonded using adhesive onto the surface of the core. Because there is no need for an adhesive film in the X-cor configuration compared to Nomex honeycomb cores, the X-cor has weight reduction superiority for use in aerospace applications.

Marascoa et al.[131] studied the failure modes of both Z-pinned sandwich panels. The failure modes were characterized by pin pull-out (in X-Cor), pin end debond (K-Cor), and shear failure by rotation of the pins. The displacement of the pin tips determines the extent of the opening of the specimen in a shear load. Rice et al.[132] demonstrated that pin-reinforced panels outperform other sandwich structures in both stiffness and load carrying capacity. A failure mode map was developed for the initial failure of a simply supported sandwich beam subject to three-point bending that displayed the different failure regions of the beam. The indentation and core shear failure were identified as the primary modes of failure of the sandwich beam. Although typical panels usually fail in the face sheets, the recent developments in optimization of panels for weight efficiency have made the face sheet failure less dominant.[133] The mechanical behavior of stitched sandwich structures has been analytically approached by Lascoup et al.[134] For both X-Cor and K-Cor truss structures, the truss transfers some of the through-thickness and shear loads improving the properties of the core.[135] X-Cortruss sandwiches were tested in three-point bending, uniaxial tension, and combined tension and bending by Kevin et al.[130]

The advantages of stitched and Z-pin foam cores are the higher shear properties compared to traditional foams. To study the crack propagation of stitched and Z-pin foam cores and the effect of adding stitches, four-point bending, core shear, and flatwise compression tests were performed, with particular attention given to the failure modes due to the presence of the stitches.[136] The rigidity and ultimate stress were shown to be higher than typical panels. Although the stitches rigidified the panels, the structure showed a brittle failure and a fragile rupture.[104]

The studies on delamination of pinned laminates have clearly shown that pins play a major role in slowing and even preventing crack propagation.[137] In order to study the effect of through-core pinning on crack behavior in sandwich structures, preliminary crack propagation tests have been conducted using a Double Cantilever Beam (DCB) specimen subject to mode-I loading. The crack propagated at mid-thickness in a symmetrical manner in the foam without pins, while in the K-Cor specimen the initial crack did not propagate and a damage zone existed near the lower core/facing interface. A considerably higher energy is required to propagate a crack in the pinned foam compared to conventional panels. The approximate fracture energies (G_c) of the K-Cor foam was at least three times higher than that of the pure foam. An advantage of the pinned panels is that the pinning parameters can be tailored for particular applications. Significant improvements in damage resistance may be accomplished with optimization of pin material, density, angle and sandwich manufacturing conditions. Stiffness, fracture strength, and damage tolerance have been examined demonstrating that for a similar weight, all these properties can be significantly improved.[136]

4.4. Density-Graded Foam Cores

Density-graded foam cores present improvements to the mechanical properties including energy absorption and impact resistance compared to homogenous foam cores. A variety of fabrication methods have been developed for density-graded foam cores. One approach is cutting the foam cores with different density at different thickness and then bonding them together.[138] However, the density of foam cores fabricated by this method cannot be continuous, and the interface problems may emerge between the layers with different density. He et al.[139] successfully prepared the density-graded aluminum foams through the coupling of the melt foaming process and the solidification process. The cooling procedure that was carried out by spraying water at the bottom of the mold was implemented before the foam melt completely grew. A new method based on density-graded polyurethane foam precursors through investment casting was developed by Brothers and Dunand.[140] Another method for fabricating density-graded aluminum foam by erosion process was investigated by Matsumoto et al.[141] The dripping rate of NaOH solution was controlled to produce a constant decrease in the fluid level inside the capacity, where a foam sample sunk into. The continuous density-graded aluminum foam was then obtained owing to different degree of corrosion in different location. A series composite model was developed by Brothers and Dunand to describe the compressive behavior of the density-graded foam.[142] It was shown that the density-graded foam exhibited a smoothly rising plateau stress instead of a near constant one as for the conventional foams. The analytical model developed by Zhang et al.[143] to characterize the low-velocity impact response of multilayer foam sandwich beams under bending load provides the theoretical basis for the graded foam structures. The theoretical model for the impact resistance and energy absorption of the graded foam rod with non-linear density gradient profiles impinged by a mass projectile was presented by Liu et al.[144] The impact resistance and energy absorption capacity of foam cores can be improved by using proper nonlinear density-graded profiles. The high-velocity crushing behavior of the density-graded foam was modeled with shock theory and the energy absorption of the foam subjected to blast loading was theoretically investigated.[145] The density-graded and homogenous foams were also analyzed numerically and experimentally under blast loading, which shows that the density-graded foams have the better blast resistance and energy absorption performance.[146–148] The experiments conducted by Nia and Kazemi showed that the increasing ballistic resistance could be obtained by using the density-graded cores.[138] Lee et al. studied the fracture behaviors of the density-graded foams by finite element method based on micromechanical model, which demonstrated that the fracture toughness of density-graded foams mainly depended on the relative density at the crack-tip.[149]

4.5. Foam Cores with Negative Poisson's Ratio

Lakes et al.[150,151] discovered that isotropic auxetic foams could be easily manufactured from conventional polyurethane open-cell foams and then the idealized re-entrant unit cell produced by symmetrical collapse of a 24-sided polyhedron. Experimental observations of negative bulk modulus in pre-strained foam were presented and analyzed. A constrained microscopic model which exhibits negative compressibility was proposed by Lakes et al.[152] Brandel et al.[153] pointed that negative Poisson's ratio was implemented by the re-entrant structures fabricated by various polyethylene foams subject to thermo-mechanical processing. After transformation from conventional foams to re-entrant structures for large cell foams (cell sizes of 1 and 2 mm), negative Poisson's ratio was exhibited over a range of processing times and temperatures, and the Poisson's ratio versus strain behavior for these foams was similar to that for reticulated polyurethane foams. Microcellular polyethylene foam was densified but cells remained convex after transformation with no substantial negative Poisson's ratio. The foam had a different transition temperature (as determined via DSC) than large cell foams.

4.6. Multifunctional Foam Cores

Various forms of multifunctional structures are being used in aerospace industry, and more and more efforts have been made to improve their performance. Kothari et al.[154] designed and analyzed a composite sandwich beam with cavities to embed avionics and integrated cooling systems with heat pipes and thermal interface materials. A sandwich beam with electronics embedded in it reduced the overall weight of a vehicle because most of the avionics housing, cables, and interconnects are no longer necessary. Cavities were maintained in the foam core of the sandwich beam to embed avionics. Various methods of reinforcement have been presented to alleviate the degradation of strength of the structure due to the presence of these cavities. The heat dissipating system consisted of thermal interface materials and a highly efficient heat transfer device designed to protect the structure from excessive thermal loads. A thermal interface composite material consisting of copper particles and a silicon matrix were proposed. Among various configurations, one using heat pipes was chosen as the preferred heat transfer device. The proposed application was an unmanned aircraft skin that acts as a radiator to maintain the embedded electronic devices within their operating temperature limit at subsonic air speeds.

5. Perspectives and Conclusions

Fabrication methods for sandwich structures with prismatic and foam-based cores still remain to be studied, especially those with a fiber-reinforced honeycomb core, which is mainly manufactured by interlocking. Common sandwich structures including corrugated-based, honeycomb-based, foam-based, and hybrid are yet to meet industry requirements for light weight, high stiffness, and high strength. New types of sandwich structures should be extended and developed to meet these demands. Multifunctionality is a promising method for further weight reduction in the aerospace, automobile, and ship industries. A promising avenue to achieve multifunctionality is by embedding functional devices and materials in the sandwich structure, given the high porosity of the core.

In this review article, recent developments in sandwich structures with corrugated, honeycomb and foam core construction were summarized. For all the three core constructions, advances in the core-face reinforcement along with the improvements and tailoring of mechanical properties were discussed. Innovative designs, manufacturing techniques and related technologies that led to a novel category of advanced core materials were highlighted. In addition, the characterization methods and the state-of-the-art processing techniques for advanced corrugated, honeycomb and foam cores were reviewed, and their limitations underlined.

Acknowledgements

The present work was partially supported by the Major State Basic Research Development Program of China (973 Program) under grant No. 2011CB610303, and by the National Science Foundation of China under grant No. 11302060. JX also gratefully acknowledged support by the Natural Scientific Research Innovation Foundation in Harbin Institute of Technology (HIT.NSRIF.2014025) and an Open-ended Fund of Science and Technology on Advanced Composites in Special Environments Laboratory. D.M., J.N., and A.V. acknowledged support by the United States National Science Foundation through grant award NSF-CMMI #1634560.

Conflict of Interest

The authors declare no conflict of interest.

Keywords

corrugated, foam, honeycomb, mechanical performance, sandwich structures

Received: January 10, 2018
Revised: August 20, 2018
Published online:

[1] C. Sennewald, S. Kaina, D. Weck, A. Gruhl, M. Thieme, G. Hoffmann, G. Stephani, R. Böhm, C. Cherif, O. Andersen, B. Kieback, W. A. Hufenbach, *Adv. Eng. Mater.* **2014**, *16*, 1234.
[2] Y. Sun, L.-C. Guo, T.-S. Wang, S.-Y. Zhong, H.-Z. Pan, *Compos. Struct*. **2018**, *185*, 446.
[3] V. Birman, G. A. Kardomateas, *Compos. Part B-Eng*. **2018**, *142*, 221.
[4] T. Lu, L. Valdevit, A. Evans, *Prog. Mater. Sci*. **2005**, *50*, 789.
[5] A. G. Evans, J. W. Hutchinson, N. A. Fleck, M. F. Ashby, H. N. G. Wadley, *Prog. Mater. Sci*. **2001**, *46*, 309.
[6] J. Xiong, R. Mines, R. Ghosh, A. Vaziri, L. Ma, A. Ohrndorf, H.-J. Christ, L. Wu, *Adv. Eng. Mater.* **2015**, *17*, 1253.
[7] B. Han, Z.-J. Zhang, Q.-C. Zhang, Q. Zhang, T. J. Lu, B.-H. Lu, *Extreme Mech. Lett*. **2017**, *10*, 58.
[8] J. Elsing, A. Quell, C. Stubenrauch, *Adv. Eng. Mater.* **2017**, *19*, 1700195.
[9] J. Banhart, H. W. Seeliger, *Adv. Eng. Mater.* **2008**, *10*, 793.
[10] A. J. Malcom, M. T. Aronson, V. S. Deshpande, H. N. G. Wadley, *Compos. Part A-Appl. S*. **2013**, *54*, 88.
[11] S. Kazemahvazi, D. Tanner, D. Zenkert, *Compos. Sci. Technol*. **2009**, *69*, 920.
[12] F. Han, Y. Yan, J. Ma, *Polym. Compos*. **2018**, *39*, 624.
[13] D.-S. Li, N. Jiang, L. Jiang, C.-Q. Zhao, *Fiber Polym*. **2016**, *17*, 460.
[14] X. Fan, I. Verpoest, J. Pflug, D. Vandepitte, P. Bratfisch, *J. Sandwich Struct. Mater.* **2009**, *11*, 179.
[15] X. Fan, I. Verpoest, J. Pflug, D. Vandepitte, P. Bratfisch, *J. Sandwich Struct. Mater.* **2009**, *11*, 151.
[16] Q. Q. Wu, Y. Gao, X. Y. Wei, D. Mousanezhad, L. Ma, A. Vaziri, J. Xiong, *Int. J. Solids Struct*. **2018**, *132–133*, 171.
[17] A. Lebée, K. Sab, *Int. J. Solids Struct*. **2010**, *47*, 2620.
[18] B. Han, Z.-J. Zhang, Q.-C. Zhang, Q. Zhang, T. J. Lu, B.-H. Lu, *Extreme Mech. Lett*. **2017**, *10*, 58.
[19] F. W. Wang, *J. Mech. Phys. Solids* **2018**, *114*, 303.
[20] L. Yang, H. Fan, J. Liu, Y. Ma, Q. Zheng, *Mater. Des*. **2013**, *50*, 863.
[21] J. Banhart, F. García-Moreno, K. Heim, H. W. Seeliger, presented at Int. Symp. Light Weighting Def., Goa, November, **2017**.
[22] T. A. Schaedler, W. B. Carter, *Annu. Rev. Mater. Res*. **2016**, *46*, 187.
[23] K.-J. Kang, *Prog. Mater. Sci*. **2015**, *69*, 213.
[24] I. Dayyani, M. I. Friswell, S. Ziaei-Rad, E. I. S. Flores, *Compos. Struct*. **2013**, *104*, 281.
[25] T. S. Jang, D. S. Oh, J. K. Kim, K. I. Kang, W. H. Cha, S. W. Rhee, *Acta Astronaut*. **2011**, *68*, 240.
[26] C. Thill, J. A. Etches, I. P. Bond, K. D. Potter, P. M. Weaver, *Smart Mater. Struct*. **2010**, *19*, 124009.
[27] C. Thill, J. D. Downsborough, S. J. Lai, *Aeronaut. J*. **2010**, *114*, 237.
[28] F. Jin, H. Chen, L. Zhao, H. Fan, C. Cai, N. Kuang, *Compos. Struct*. **2013**, *98*, 53.
[29] G. Kooistra, V. Deshpande, H. Wadley, *J. Appl. Mech*. **2007**, *74*, 259.
[30] C. Kılıçaslan, İ. K. Odacı, M. Güden, *J. Sandwich. Struct. Mater.* **2016**, *18*, 667.
[31] M. Leekitwattana, S. W. Boyd, R. A. Shenoi, *J. Constr. Steel Res*. **2011**, *67*, 248.
[32] D. Y. Seong, C. G. Jung, D. Y. Yang, K. J. Moon, D. G. Ahn, *Mater. Des*. **2010**, *31*, 2804.
[33] A. Malcom, H. Wadley, B. Russell, *J. Mech. Mater. Struct*. **2010**, *5*, 477.
[34] S. Kazemahvazi, N. Khokar, S. Hallstrom, H. N. G. Wadley, V. S. Deshpande, *Compos. Sci. Technol*. **2016**, *127*, 95.
[35] A. J. Malcom, M. T. Aronson, H. N. G. Wadley, *J. Compos. Mater.* **2015**, *50*, 25.
[36] S. Kazemahvazi, D. Zenkert, *Compos. Sci. Technol*. **2009**, *69*, 913.
[37] L. Valdevit, Z. Wei, C. Mercer, F. W. Zok, A. G. Evans, *Int. J. Solids Struct*. **2006**, *43*, 4888.
[38] S. R. Atashipour, M. Al-Emrani, *Int. J. Solids Struct.* **2017**, *129*, 1.
[39] Y. Yu, W. B. Hou, P. Hu, L. Ying, G. Akhmet, *Compos. Struct*. **2017**, *176*, 449.
[40] B. T. Cao, B. Hou, Y. L. Li, H. Zhao, *Int. J. Solids Struct*. **2017**, *109*, 33.
[41] S. Heimbs, P. Middendorf, S. Kilchert, A. F. Johnson, M. Maier, *Appl. Compos. Mater.* **2007**, *14*, 363.
[42] A. A. Razdaibedin, V. I. Khaliulin, *Russ. Aeronaut*. **2015**, *58*, 88.
[43] Y. C. Zhang, Z. L. Wang, S. L. Zhang, G. J. Zhai, *Ship Eng*. **2009**, *31*, 1.
[44] B. B. Basily, E. A. Elsayed, *Int. J. Mater. Prod. Technol*. **2004**, *21*, 169.
[45] S. Fischer, K. Drechsler, S. Kilchert, A. Johnson, *Compos. Part A-Appl. S*. **2009**, *40*, 1941.
[46] J. M. Gattas, Z. You, *Int. J. Solids Struct*. **2015**, *53*, 80.
[47] S. Heimbs, J. Cichosz, M. Klaus, S. Kilchert, A. F. Johnson, *Compos. Struct*. **2010**, *92*, 1485.
[48] S. H. Yoo, S. H. Chang, M. P. F. Sutcliffe, *Compos. Part A-Appl. S*. **2010**, *41*, 427.
[49] C. W. Schwingshackl, G. S. Aglietti, P. R. Cunningham, *AIAA J*. **2007**, *45*, 491.
[50] C. W. Schwingshackl, G. S. Aglietti, P. R. Cunningham, *AIAA J*. **2006**, *44*, 2286.
[51] F. Gandhi, P. Anusontiinthra, *Smart Mater. Struct*. **2008**, *17*, 1343.
[52] I. Dayyani, S. Ziaei-Rad, H. Salehi, *Appl. Compos. Mater.* **2012**, *19*, 705.
[53] I. Dayyani, S. Ziaei-Rad, M. I. Friswell, *J. Compos. Mater.* **2013**, *48*, 1623.
[54] M. Yamashita, M. Gotoh, *Int. J. Impact Eng*. **2005**, *32*, 618.
[55] D. Han, S. W. Tsai, *J. Compos. Mater.* **2003**, *37*, 287.
[56] S. Kelsey, R. A. Gellatly, B. W. Clark, *Aircr. Eng*. **1958**, *30*, 294.
[57] H. L. Fan, F. H. Meng, W. Yang, *Arch. Appl. Mech*. **2006**, *75*, 635.
[58] H. L. Fan, F. H. Meng, W. Yang, *Compos. Struct*. **2007**, *81*, 533.
[59] B. P. Russell, V. S. Deshpande, H. Wadley, *J. Mech. Mater. Struct*. **2008**, *3*, 1315.
[60] B. P. Russell, T. Liu, N. A. Fleck, V. S. Deshpande, *J. Appl. Mech*. **2011**, *78*, 2388.
[61] A. Matzenmiller, J. Lubliner, R. L. Taylor, *Mech. Mater.* **1995**, *20*, 125.
[62] Z. Hashin, *J. Appl. Mech*. **1980**, *47*, 329.
[63] J. Fazilati, M. Alisadeghi, *Thin Wall Struct*. **2016**, *107*, 197.
[64] G. Palomba, G. Epasto, V. Crupi, E. Guglielmino, *Int. J. Impact Eng*. **2018**, *121*, 77.
[65] A. Ajdari, B. H. Jahromi, J. Papadopoulos, H. Nayeb-Hashemi, A. Vaziri, *Int. J. Solids Struct*. **2012**, *49*, 1413.
[66] A. Vigliotti, D. Pasini, *Mech. Mater.* **2013**, *62*, 32.
[67] Q. Chen, N. Pugno, K. Zhao, Z. Y. Li, *Compos. Struct*. **2014**, *109*, 68.
[68] J. J. Zheng, L. Zhao, H. Fan, *Compos. Part B-Eng*. **2012**, *43*, 1516.
[69] L. Zhao, Q. Zheng, H. Fan, F. Jin, *Mater. Des*. **2012**, *40*, 124.
[70] Y. Liu, H. Hu, *Sci. Res. Essays* **2010**, *5*, 1052.
[71] Z. Y. Ge, H. Hu, *Text. Res. J*. **2012**, *83*, 543.
[72] H. Hu, Z. Wang, S. Liu, *Text. Res. J*. **2011**, *81*, 1493.
[73] Y. P. Liu, H. Hu, J. K. C. Lam, S. Liu, *Text. Res. J*. **2010**, *80*, 856.
[74] D. Li, J. H. Yin, L. Dong, R. S. Lakes, *J. Mater. Sci*. **2018**, *53*, 3493.
[75] A. Alderson, K. L. Alderson, D. Attard, K. E. Evans, R. Gatt, J. N. Grima, W. Miller, N. Ravirala, C. W. Smith, K. Zied, *Compos. Sci. Technol*. **2010**, *70*, 1042.
[76] W. J. Zhang, R. Neville, D. Zhang, F. Scarpa, L. Wang, R. Lakes, *Int. J. Solids Struct*. **2018**, *141–142*, 254.
[77] L. Mizzi, E. M. Mahdi, K. Titov, R. Gatt, D. Attard, K. E. Evans, J. N. Grima, J.-C. Tan, *Mater. Des*. **2018**, *146*, 28.
[78] J. X. Qiao, C. Q. Chen, *Int. J. Impact Eng*. **2015**, *83*, 47.
[79] J. X. Qiao, C. Q. Chen, *J. Appl. Mech*. **2015**, *82*, 51007.
[80] L. Yang, O. Harrysson, H. West, D. Cormier, *Int. J. Solids Struct*. **2015**, *69–70*, 475.
[81] M. Fu, F. M. Liu, L. L. Hu, *Compos. Sci. Technol*. **2018**, *160*, 111.
[82] X.-T. Wang, B. Wang, Z.-H. Wen, L. Ma, *Compos. Sci. Technol*. **2018**, *164*, 92.
[83] Y. Y. Xue, X. F. Wang, W. Wang, X. K. Zhong, F. Han, *Mater. Sci. Eng. A* **2018**, *722*, 255.

[84] T. T. Li, Y. Y. Chen, X. Hu, Y. Li, L. Wang, *Mater. Des*. **2018**, *142*, 247.
[85] X.-T. Wang, X.-W. Li, L. Ma, *Mater. Des*. **2016**, *99*, 467.
[86] M. Mir, M. Ali, U. Ansari, J. Sami, *Adv. Mater. Sci. Eng*. **2014**, *2014*, 753496.
[87] V. H. Carneiro, J. Meireles, H. Puga, *Mater. Sci. —Poland* **2013**, *31*, 561.
[88] Y. Jiang, Z. Y. Liu, N. Matsuhisa, D. P. Qi, W. R. Leow, H. Yang, J. Yu, G. Chen, Y. Liu, C. Wan, Z. J. Liu, X. D. Chen, *Adv. Mater*. **2018**, *30*, 1706589.
[89] T. C. Lim, A. Alderson, K. L. Alderson, *Phys. Status Solidi B* **2014**, *251*, 307.
[90] J. Summers, D. Marcelli, B. Neudecker, *Collect. Tech. Pap. – AIAA/ASME/ASCE/AHS Struct., Struct. Dyn. Mater. Conf*. **2013**, *2002–1242*, 22.
[91] B. J. Neudecker, M. H. Benson, B. K. Emerson, presented at 14th Int. Conf. Compos. Mater., San Diego, July, **2003**.
[92] P. Bollen, N. Quiévy, I. Huynen, C. Bailly, C. Detrembleur, J. M. Thomassin, T. Pardoen, *Scr. Mater*. **2013**, *68*, 50.
[93] P. C. Kim, D. G. Lee, *Compos. Struct*. **2009**, *87*, 161.
[94] K. Park, S. Lee, C. Kim, J. Han, *Compos. Sci. Technol*. **2006**, *66*, 576.
[95] H. L. Fan, W. Yang, Z. M. Chao, *Compos. Sci. Technol*. **2007**, *67*, 3472.
[96] M. Chen, Y. M. Pei, D. Fang, *Appl. Phys. A: Mater. Sci. Process* **2012**, *108*, 75.
[97] M. Chen, Y.-M. Pei, D.-N. Fang, *Appl. Math. Mech*. **2010**, *31*, 339.
[98] M. Chen, Y. M. Pei, D. Fang, *Comp. Mater. Sci*. **2009**, *46*, 591.
[99] M. Chen, Y. M. Pei, D. Fang, *Int. J. Appl. Electromagn. Mech*. **2010**, *33*, 1691.
[100] K. R. Olympio, F. Gandhi, *J. Intell. Mater. Syst. Strruct*. **2010**, *21*, 1719.
[101] D. Schwingel, H.-W. Seeliger, C. Vecchionacci, D. Alwes, J. Dittrich, *Acta Astronaut*. **2007**, *61*, 326.
[102] J. Banhart, H.-W. Seeliger, *Adv. Eng. Mater*. **2012**, *14*, 1082.
[103] J. H. Kim, Y. S. Lee, B. J. Park, D. H. Kim, *Compos. Struct*. **1999**, *47*, 543.
[104] B. Lascoup, Z. Aboura, K. Khellil, M. Benzeggagh, *Compos. Sci. Technol*. **2006**, *66*, 1385.
[105] S. Ai, Y. Mao, Y. M. Pei, D. Fang, L. Tang, *Mater. Des*. **2013**, *50*, 817.
[106] B. Lascoup, Z. Aboura, K. Khellil, M. Benzeggagh, *Compos. Struct*. **2010**, *92*, 347.
[107] F. Xia, X.-Q. Wu, *Compos. Struct*. **2010**, *92*, 412.
[108] F. Zhu, C. C. Chou, K. H. Yang, *Compos. Part B-Eng*. **2011**, *42*, 1202.
[109] Y. Sun, Q. M. Li, *Int. J. Impact Eng*. **2018**, *112*, 74.
[110] A. G. Hanssen, L. Enstock, M. Langseth, *Int. J. Impact Eng*. **2002**, *27*, 593.
[111] F. Zhu, Z. Wang, G. Lu, L. M. Zhao, *Mater. Des*. **2009**, *30*, 91.
[112] F. Zhu, L. M. Zhao, G. X. Lu, Z. H. Wang, *Adv. Struct. Eng*. **2016**, *11*, 525.
[113] Y. Sun, Q. M. Li, T. Lowe, S. A. McDonald, P. J. Withers, *Mater. Des*. **2016**, *89*, 215.
[114] S. A. Tekalur, A. E. Bogdanovich, A. Shukla, *Compos. Sci. Technol*. **2009**, *69*, 736.
[115] J. Guilleminot, S. Comas-Cardona, D. Kondo, C. Binetruy, P. Krawczak, *Compos. Sci. Technol*. **2008**, *68*, 1777.
[116] S. G. Ai, Y. Mao, Y. M. Pei, D. Fang, L. Tang, *Compos. Struct*. **2013**, *99*, 41.
[117] M. V. Hosur, M. Abdullah, S. Jeelani, *Compos. Struct*. **2004**, *65*, 103.
[118] M. V. Hosur, M. Abdullah, S. Jeelani, *Compos. Struct*. **2005**, *69*, 167.
[119] A. Corigliano, E. Rizzi, E. Papa, *Compos. Sci. Technol*. **2000**, *60*, 2169.
[120] C. Liu, D. A. Cai, G. M. Zhou, F. Z. Lu, *Appl. Compos. Mater*. **2017**, *24*, 1151.
[121] A. S. Vaidya, U. K. Vaidya, N. Uddin, *Mater. Sci. Eng. A* **2008**, *472*, 52.
[122] M. V. Hosur, M. Abdullah, S. Jeelani, *Mater. Sci. Eng. A* **2007**, *445–446*, 54.
[123] H. Judawisastra, J. Ivens, I. Verpoest, *Compos. Struct*. **1998**, *43*, 35.
[124] A. W. V. Vuure, J. Pflug, J. A. Ivens, I. Verpoest, *Compos. Sci. Technol*. **2000**, *60*, 1263.
[125] A. Henao, M. Carrera, A. Miravete, L. Castejón, *Compos. Struct*. **2010**, *92*, 2052.
[126] X. T. Zheng, J. F. Zhang, F. Yang, *Adv. Mater. Res*. **2008**, *33–37*, 477.
[127] P. Wang, Y. Lei, Z. F. Yue, *Compos. Struct*. **2013**, *100*, 243.
[128] T. Lu, L. Valdevit, A. Evans, *Prog. Mater. Sci*. **2005**, *50*, 789.
[129] A. G. Evans, J. W. Hutchinson, N. A. Fleck, M. F. Ashby, H. N. G. Wadley, *Prog. Mater. Sci*. **2001**, *46*, 309.
[130] T. K. O'Brien, I. L. Paris, *Compos. Struct*. **2002**, *57*, 189.
[131] A. I. Marasco, D. D. R. Cartié, I. K. Partridge, A. Rezai, *Compos. Part A-Appl. S*. **2006**, *37*, 295.
[132] M. C. Rice, C. A. Fleischer, M. Zupan, *Exp. Mech*. **2006**, *46*, 197.
[133] C. A. Steeves, N. A. Fleck, *Int. J. Mech. Sci*. **2004**, *46*, 561.
[134] B. Lascoup, Z. Aboura, K. Khellil, M. Benzeggagh, *Compos. Sci. Technol*. **2010**, *70*, 350.
[135] D. D. Cartié, N. A. Fleck, *Compos. Sci. Technol*. **2003**, *63*, 2401.
[136] B. Lascoup, Z. Aboura, K. Khellil, M. Benzeggagh, *Sandwich Structures 7: Advancing with Sandwich Structures and Materials*, Springer, Netherlands **2005**, p. 681.
[137] I. K. Partridge, D. D. R. Cartié, *Compos. Part A-Appl. S*. **2005**, *36*, 55.
[138] A. A. Nia, M. Kazemi, *J. Sandwich Struct. Mater*. **2018**, https://doi.org/10.1177/1099636218757669
[139] S.-Y. He, Y. Zhang, G. Dai, J.-Q. Jiang, *Mater. Sci. Eng. A* **2014**, *618*, 496.
[140] A. H. Brothers, D. C. Dunand, *Adv. Eng. Mater*. **2006**, *8*, 805.
[141] Y. Matsumoto, A. H. Brothers, D. C. Dunand, *Mater. Sci. Forum* **2007**, *539–543*, 1903.
[142] A. H. Brothers, D. C. Dunand, *Mater. Sci. Eng. A* **2008**, *489*, 439.
[143] J. X. Zhang, Q. H. Qin, S. J. Chen, Y. Yang, Y. Ye, C. P. Xiang, T. J. Wang, *J. Sandwich Struct. Mater*. **2018**, https://doi.org/10.1177/1099636218759827
[144] H. Liu, Z. Q. Zhang, H. Liu, J. Yang, H. Lin, *Compos. Part B-Eng*. **2017**, *116*, 76.
[145] H. Y. Zhou, Y. H. Wang, X. J. Wang, Z. Zhao, G. W. Ma, *Mater. Des*. **2015**, *84*, 351.
[146] Y. Xia, C. Q. Wu, Z.-X. Liu, Y. Yuan, *Constr. Build. Mater*. **2016**, *111*, 209.
[147] L. Jing, L. M. Zhao, *J. Sandwich Struct. Mater*. **2017**, https://doi.org/10.1177/1099636217695651
[148] J. Li, G. W. Ma, H. Y. Zhou, X. Du, *Int. J. Prot. Struct*. **2011**, *2*, 333.
[149] S.-J. Lee, J. Q. Wang, B. V. Sankar, *Int. J. Solids Struct*. **2007**, *44*, 4053.
[150] E. A. Friis, R. S. Lakes, J. B. Park, *J. Mater. Sci*. **1988**, *23*, 4406.
[151] R. Lakes, *Science* **1987**, *235*, 1038.
[152] R. Lakes, K. W. Wojciechowski, *Phys. Status Solidi B* **2008**, *245*, 545.
[153] B. Brandel, R. S. Lakes, *J. Mater. Sci*. **2001**, *36*, 5885.
[154] R. Kothari, C. T. Sun, *J. Sandwich Struct. Mater*. **2012**, *14*, 734.

